



UPPSALA
UNIVERSITET

*Digital Comprehensive Summaries of Uppsala Dissertations
from the Faculty of Science and Technology 890*

From 2D to 3D Models of Electrical Conductivity based upon Magnetotelluric Data

Experiences from two Case Studies

JULIANE HÜBERT



ACTA
UNIVERSITATIS
UPSLIENSIS
UPPSALA
2012

ISSN 1651-6214
ISBN
[urn:nbn:se:uu:diva-165143](http://urn.nbn.se/uu:diva-165143)

Dissertation presented at Uppsala University to be publicly examined in Hambergsalen, Geocentrum, Villavägen 16, Uppsala. Friday, February 17, 2012 at 10:00 for the degree of Doctor of Philosophy. The examination will be conducted in English.

Abstract

Hübert, J. 2012. From 2D to 3D Models of Electrical Conductivity based upon Magnetotelluric Data: Experiences from two Case Studies. *Acta Universitatis Upsaliensis. Digital Comprehensive Summaries of Uppsala Dissertations from the Faculty of Science and Technology* 890. 55 pp. Uppsala.

Magnetotelluric measurements are among the few geophysical techniques capable of imaging the structure both in the shallow subsurface as well as the entire crust of the Earth. With recent technical and computational advances it has become possible to derive three-dimensional inversion models of the electrical conductivity from magnetotelluric data, thereby overcoming the problems arising from the simplified assumption of two-dimensionality in conventional two-dimensional modeling. The transition from two-dimensional to three-dimensional analysis requires careful reconsideration of the classical challenges of magnetotellurics: galvanic distortion, data errors, model discretization and resolution. This work presents two examples of magnetotelluric investigations, where a new three-dimensional inversion algorithm has been applied. The new models are compared with conventional two-dimensional models and combined with the results of other geophysical techniques like reflection seismics and electrical resistivity tomography. The first case presents magnetotelluric investigations of the Kristineberg mining area in the Skellefte district, northern Sweden. This study is part of a joint geophysical and geological project to investigate the present structure and evolution of the whole district. Together with reflection seismic and surface geological information a three-dimensional conductivity model, derived through the inversion of magnetotelluric data, was interpreted. A comparison with two-dimensional modeling gives insights into the capabilities and challenges of three-dimensional inversion strategies with respect to data sampling and model resolution. The second case presents a study of remediation monitoring with geophysical methods after an oil blow-out in Trecate, Italy. A three-dimensional conductivity model was derived from radiomagnetotelluric measurements. In addition, two-dimensional joint inversion of radiomagnetotelluric and electrical tomography data was performed. Compared with electrical resistivity tomography, radiomagnetotelluric data is more sensitive to conductors and the derived three-dimensional inversion model resolves the vadose zone and the underlying aquifer.

Juliane Hübert, Uppsala University, Department of Earth Sciences, Geophysics, Villav. 16, SE-752 36 Uppsala, Sweden.

© Juliane Hübert 2012

ISSN 1651-6214

urn:nbn:se:uu:diva-165143 (<http://urn.kb.se/resolve?urn=urn:nbn:se:uu:diva-165143>)

List of papers

This thesis is based on the following papers, which are referred to in the text by their Roman numerals.

- I **J. Hübert**, A. Malehmir, M. Smirnov, A. Tryggvason, and L. B. Pedersen (2009). MT measurements in the western part of the Paleoproterozoic Skellefte Ore District, Northern Sweden: A contribution to an integrated geophysical study. *Tectonophysics* 475(3-4), 493 - 502.
- II M. d. A. García Juanatey, **J. Hübert**, A. Tryggvason and L. B. Pedersen, 2011. Imaging the Kristineberg mining area with two perpendicular magnetotelluric profiles in the Skellefte Ore District, northern Sweden. *Geophysical prospecting* (in press).
- III **J. Hübert**, M. d. A. García Juanatey, A. Malehmir, M. Smirnow, A. Tryggvason, and L. B. Pedersen: Upper crustal resistivity structure of the Kristineberg area, Skellefte district, northern Sweden with 3D magnetotellurics. Submitted to *Geophysical journal international*
- IV M. Bastani, **J. Hübert**, T. Kalscheuer, L. B. Pedersen, A. Godino and J. Bernard: 2D joint inversion of RMT and ERT data versus individual 3D inversion of full tensor RMT data. An example from the Trecale site in Italy. Submitted to *Geophysics*

Reprints were made with permission from the publishers.

For paper II, J. H. performed the 3D synthetic study and assisted during data acquisition, processing and interpretation.

For paper IV, J. H. performed the 3D inversion of the data, the synthetic study and wrote parts of the manuscript.

A publication that is not included in the thesis:

- Pedersen, L., **Hübert, J.**, and Dynesius, L. (2010). Controlled Source Radio Magnetotellurics (CSRMT) with an electric dipole. Technical report, Geological Survey of Sweden.

Contents

1	Introduction	7
2	Electromagnetic methods	9
2.1	Electromagnetic theory	10
2.2	Magnetotellurics and Geomagnetic Depth Sounding	11
2.2.1	Fundamentals	11
2.2.2	Data acquisition and processing	12
2.3	Dimensionality and distortion	13
2.3.1	Distortion model and strike analysis	14
2.3.2	Static shift corrections	16
2.3.3	VMTs in 2D and 3D	17
3	Inversion and forward modeling of MT data	19
3.1	Forward modeling of EM fields	19
3.2	Inversion of MT data	20
3.2.1	2D and 3D MT inversion algorithms	21
3.3	MT in combination with other geophysical methods	23
4	Introduction to the field areas	25
4.1	Kristineberg, western Skellefte district, northern Sweden	25
4.2	Trecate site, Italy	28
5	Summary of papers	31
5.1	MT measurements in the western part of the Paleoproterozoic Skellefte Ore District, Northern Sweden: A contribution to an integrated geophysical study.	31
5.2	Imaging the Kristineberg mining area with two perpendicular magnetotelluric profiles in the Skellefte Ore District, northern Sweden.	33
5.3	Upper crustal resistivity structure of the Kristineberg area, Skellefte district, northern Sweden revealed by 3D magnetotellurics.	37
5.4	2D joint inversion of RMT and ERT data versus individual 3D inversion of full tensor RMT data. An example from the Trecate site in Italy.	41
6	Discussion and conclusions	45
	Sammanfattning på svenska	47
	Acknowledgments	50
	References	52

1. Introduction

Geophysical techniques uniquely enable an insight into the structure of the earth by surface observations. The magnetotelluric (MT) method uses the ingenious concept of deducing the electrical resistivity structure - which is coupled to the geometry, composition and physical properties of the subsurface - from the natural variations of the electromagnetic field measured at the surface. The concept finds its applications in all types of geological settings like plate boundaries, fault zones, volcanic regions as well as in the exploration of mineral resources. It is used for hydrogeological investigations, archaeological studies and waste disposal monitoring, using integrated interpretation and joint inversion with information from other geophysical and geological observations. Due to recent advances in instrumentation, processing algorithms and computational power it has become feasible to resolve the subsurface in all three dimensions. 3D inversion techniques are used to mathematically derive models of the electrical resistivity that represent structures in the ground from time series recordings of electromagnetic field components. The transition from 2D to 3D inversion in the last decade is a huge leap in science. 3D inversion is far from being a standard procedure, reflected in the limited amount of literature up to this date. There has been rapid and extensive developments in the past years, but those tools are not publicly available. Nowadays challenges are the computational complexity, the continuous evaluation of galvanic distortion effects on the observed data as well as model assessment.

The course of this thesis is as follows:

Paper I describes a typical 2D MT case study with collocated seismic interpretation from the Kristineberg area in the Skellefte district in northern Sweden. 20 BMT sites were collected along a 20 km long profile perpendicular to an assumed strike direction. After a dimensionality analysis, 2D inversion was carried out and a stable electrical conductivity model of the upper 12 km could be derived. Electrical features in the model are correlated with different zones of seismic reflectivity and interpreted as lithological units known from surface observations. The results contain important aspects for the understanding of the processes that shaped the present day Skellefte district.

Paper II continues the investigations of the Kristineberg area with additional BMT measurements closer to the mine with sites on two ca. 10 km long perpendicular profiles. We encountered the typical challenges of the 2D assumption of how to define a common geoelectric strike direction. Thorough dimensionality analysis leads to the conclusion that the underlying resistivity distribution suffers from moderate 3D effects. Nevertheless, 2D inversion of the

impedance determinant data can still produce reasonable results. Some more enigmatic model features are addressed by model assessment techniques. To quantify the 3D effect on the data, a synthetic 3D study was performed.

Paper III concludes the electromagnetic studies in the Skellefte district by presenting a first 3D inversion model of a $20 \times 20 \text{ km}^2$ area around the Kristineberg mine. Data sampling and quality of the total 68 sites is not ideal, but the derived model is reasonable when combined with results from seismic reflection images and surface and borehole geological information. The validity of the model is assessed by forward modeling and the comparison with the previous 2D inversion results.

Paper IV leads the reader to another field area at an oil-blow-out close to Treccate, Italy. As parts of a multidisciplinary study, RMT and ERT data were collected over a densely sampled array to investigate the vadose zone of the contaminated area and the general geometry of the aquifer. A synthetic study was performed to investigate the capabilities and limitations of both methods in a single 3D RMT inversion and 2D joint RMT and ERT approach. The derived inversion models of the field data highlight the role that RMT measurements can play in a monitoring project.

2. Electromagnetic methods

Electrical resistivity, or its inverse, electrical conductivity, is a material specific parameter with a large variation between different types of rocks, that span over ten magnitudes (see Fig. 2.1). The main causes for larger areas of enhanced electrical conductivity in the earth's crust are fluids, graphite, serpentinite and partial melts, whereas in the shallower subsurface groundwater, brines or other fluids and the presence of ore bodies determine the electrical response (e.g. Hutton and Haak, 1991). This makes the estimation of electrical resistivity an excellent tool to image the subsurface. The penetration depth of electromagnetic waves and with it the depth of investigation are controlled by the frequency. As diverse as the field of applications is the variety of electrical and electromagnetic methods in geophysics in the shallower subsurface (max. 1000 m depth of investigation). Magnetotellurics (MT) however is the only technique capable of investigating the electrical structure of the upper 100 km of the earth. Its comparatively low costs during acquisition is due to the use of natural variations of the electromagnetic field in the frequency band $10^{-3} - 10^3$ Hz which are generated by processes in the atmosphere, ionosphere and magnetosphere. Artificial sources are used in controlled-source-magnetotellurics (CSMT) when signal-to-noise-ratios and frequency range of the natural signal are suboptimal for the specific application. For Radiomagnetotellurics (RMT), the signal (in the frequency range 10 – 240 kHz) of military radio and VLF transmitters, that are quite common in Europe, (Bastani and Pedersen, 2001) is used. For both the natural field MT and the RMT case, source and receiver distances are regarded as sufficiently large to neglect source effects in the signal. Plane wave incidence of the electromagnetic field can be assumed when displacement currents can be neglected.

MT has its origins in the 1950s with the pioneering work of Cagniard (1953) and Tikhonov (1950). Since those first applications that assumed a layered resistivity distribution in the Earth, theory and instrumentation have evolved immensely. With the advances of modern computers as “number crunchers” and the development of numerical algorithms, the inversion of the observed field data has become popular to derive electrical conductivity models of the subsurface. For the last two decades, 2D inversion and interpretation has been the standard.

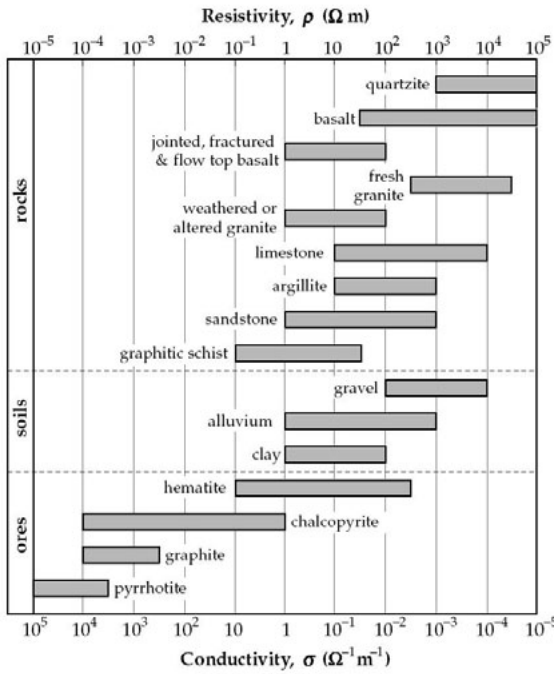


Figure 2.1. Resistivity values for different rock types, after Telford et al. (1990)

2.1 Electromagnetic theory

Maxwell's equations describe the relation between the magnetic H and the electric E fields. Essential for the magnetotelluric method are Faraday's and Ampere's law (including displacement currents) in frequency domain:

$$\nabla \times E = -(i\omega\mu)H \quad (2.1)$$

$$\nabla \times H = (\sigma + i\omega\epsilon)E + J_e \quad (2.2)$$

where ω is the angular frequency, $\mu = \mu_0\mu_r$ the product of the magnetic permeability of the medium and the magnetic constant, $\epsilon = \epsilon_0\epsilon_r$ the combination of the dielectric permittivity of the material and the dielectric constant and σ the electrical conductivity. For MT relevant cases, both ϵ and μ are assumed to be constant. J_e is the current density of an external source. Under the quasi-static approximation disregarding displacement currents, equations 2.1 and 2.2 can be transformed into differential expressions for the electric and magnetic field describing their diffusive propagation into the earth, assuming that the source is above the surface:

$$\nabla \times \nabla \times E = i\omega\mu\sigma E \quad (2.3)$$

$$\nabla \times (\rho \nabla \times H) = i\omega\mu H \quad (2.4)$$

with $\rho = \frac{1}{\sigma}$ as the electrical resistivity. These are the basis for numerical modeling of electromagnetic fields (see below). The penetration depth of the plane electromagnetic waves can be approximated in terms of the skin depth (Schmucker and Weidelt, 1975):

$$\delta = \sqrt{\frac{2\rho}{\mu\omega}} \approx 500 \cdot \sqrt{\frac{\rho}{f}}, \quad (2.5)$$

where f is the frequency and ρ some representative resistivity of the medium.

2.2 Magnetotellurics and Geomagnetic Depth Sounding

2.2.1 Fundamentals

The basic principles of the MT method were introduced by Tikhonov (1950) and Cagniard (1953). The impedance tensor Z is defined as the relation in frequency domain between the components of the magnetic field H and those of the electric field E measured at the surface of the earth for incident plane wave:

$$\begin{bmatrix} E_x \\ E_y \end{bmatrix} = \begin{bmatrix} Z_{xx} & Z_{xy} \\ Z_{yx} & Z_{yy} \end{bmatrix} \cdot \begin{bmatrix} H_x \\ H_y \end{bmatrix}, \quad (2.6)$$

indices x and y denoting magnetic North and East, μ_0 being the magnetic permeability of vacuum. Z is a complex tensor and usually displayed as apparent resistivity ρ_a and phase ϕ that depend on the angular frequency ω :

$$\rho_a(\omega) = \frac{1}{\omega\mu_0} \cdot |Z(\omega)|^2 \quad (2.7)$$

$$\phi(\omega) = \arctan \frac{\text{Im}(Z(\omega))}{\text{Real}(Z(\omega))}. \quad (2.8)$$

Simultaneously, the variation of the vertical component (z-direction) of the magnetic field is also measured. In geomagnetic depth sounding (GDS) the transfer function between vertical and horizontal magnetic fields T is calculated:

$$H_z(\omega) = T_x(\omega) \cdot H_x(\omega) + T_y(\omega) \cdot H_y(\omega). \quad (2.9)$$

T is also complex and frequency dependent and contains independent information about the conductivity distribution of the subsurface. I will refer to T as the vertical magnetic transfer function (VMT).

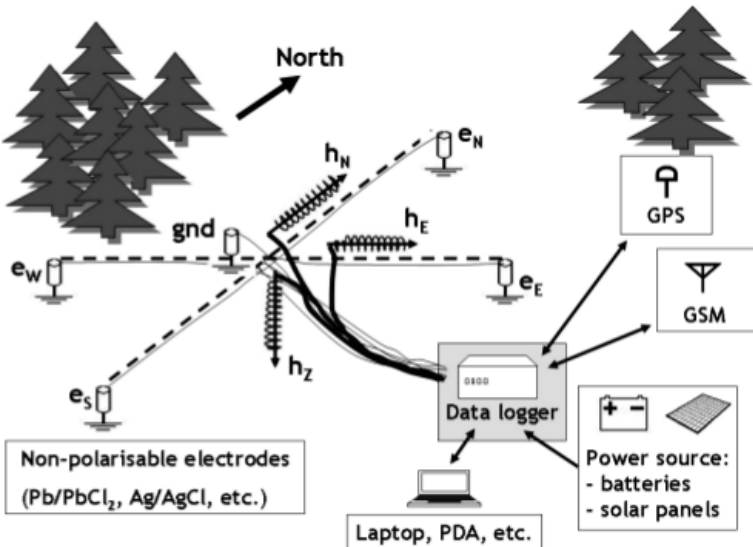


Figure 2.2. Schematic figure of a MT site installation after Smirnov et al. (2008).

2.2.2 Data acquisition and processing

For BMT measurements, Induction coil magnetometers from Metronix, Germany and Lemi, Ukraine were used to record the variation in the magnetic field. These highly sensible instruments work in a period range between 10^{-3} and several thousands seconds. Non polarizable Pb/PbCl electrodes are employed as electric sensors. All sensors are buried 50 – 100 cm during installation, a schematic setup can be seen in Fig. 2.2. Time series were recorded with GPS synchronization on an Earth data logger. The common duration of measurement was about a full day, to exploit possible increase in signal-to-noise-ratios during night hours. While the continuous sampling rate is 20 Hz, a night time burst mode was recorded with 1000 Hz during two hours after midnight when the influence of cultural noise is expected to be lower. On some occasions, an extra high frequency run with 3000 Hz was recorded. The installation of a BMT site takes 1.5 – 4 hours, heavily depending on local ground conditions. Special care has to be taken to avoid the influence of artificial electromagnetic signals from human infrastructures such as power lines and settlements. Due to the duration of the recording and the limited number of available instruments, it requires a considerable effort to collect a sufficient amount of data to allow for 3D inverse modeling. The data analyzed in paper I-III were collected in four field campaigns in 2007-2010, with three (in 2007) to six (in 2010) available instruments for simultaneous deployment. Magnetotelluric impedances and VMTs at each site were derived from the measurement of time series of the electric and magnetic fields, using the robust statistical software package *MTU2000* (Smirnov, 2003), which also allowed for remote

reference processing for simultaneous recordings. For natural source MT, time series processing is an integral and challenging part of data analysis.

RMT measurements were carried out with the EnviroMT instrument (Bastani, 2001) which consists of three induction coil magnetometers, five steel electrodes, a signal amplifier box and the processing unit. Transmitters can be selected manually. With the EnviroMT, installation and measurement at one site take only a couple of minutes, it is therefore possible to collect a lot of data in short time. The estimation of the transfer functions happens instantaneously and is an automated process (Bastani, 2001) using a truncated singular value decomposition (TSVD) technique to account for possible noise effects and the irregular distribution of transmitters in both azimuthal and frequency range. RMT is sensitive to near infrastructure, but somewhat more robust than natural source MT, when at least about 25 transmitters are available.

Real errors and error floors

Error floors are used to avoid an underestimation of the calculated measurement errors. In 2D inversion, impedances are converted to apparent resistivity and phases. The corresponding errors ($\Delta\rho_a$ and $\Delta\phi$) are:

$$\frac{\Delta\rho_a}{\rho_a} = 2 \cdot \frac{\Delta|Z|}{|Z|} \quad (2.10)$$

$$\Delta\phi = \frac{\Delta|Z|}{|Z|}. \quad (2.11)$$

E.g., 1% relative error on the impedance corresponds to 2% on apparent resistivity and 0.57° on phase data.

Gaussian errors for synthetic data are computed as absolute errors (as a percentage of the absolute value of the impedance). RMS data fits of the inversion models are always relative to the actual error used, i.e. error floor and measured errors.

2.3 Dimensionality and distortion

The impedance tensor has properties that allow implications about the dimensionality of the underlying resistivity structure. The study of these properties is essential before making simplifying assumption about the dimensionality when applying 1D or 2D inversion. Certain aspects, especially the search for a predominant “geoelectric strike” direction, become obsolete in 3D. Nevertheless, the distortion effects due to very small inhomogeneities close to the measurement locations can produce biased models and have to be taken into consideration during interpretation. The most basic description of the resistivity structure of the earth is a layered half space (or sphere for global induction studies). In this one dimensional case, the diagonal impedance elements are

zero, and the so-called main impedances are $Z_{xy} = -Z_{yx}$. In the ideal 2D case, i.e. when there is one geoelectric strike direction, the impedance tensor decouples into two modes: *E-polarization* (also referred to as TE mode) containing electric fields parallel to the strike of the lateral contrast as well as the perpendicular and the vertical component of the magnetic field, and *B-polarization* (also referred to as TM mode) including the electric field component crossing the resistivity contrast and the corresponding magnetic field component. In the correct reference frame, the diagonal elements will be zero. In reality this might not be the case due to a rotated reference frame, inductive or galvanic coupling to small scale inhomogeneities, 3D effects or data errors (noise). Therefore it is necessary to perform dimensionality and distortion analysis on the data to correctly approximate TE and TM mode by Z_{xy} and Z_{yx} before applying 2D inversion. There are several approaches on how to find the optimal strike direction and characterize distortion.

Indicators for dimensionality after Bahr (1991) were used for the impedance data in paper I and II, using: $S_1 = Z_{xx} + Z_{yy}$, $S_2 = Z_{xy} + Z_{yx}$, $D_1 = Z_{xx} - Z_{yy}$ and $D_2 = Z_{xy} - Z_{yx}$. S_1 and D_2 are rotationally invariant. Then one can define:

1. Swift skew (Swift, 1967):

$$\kappa = \frac{|S_1|}{|D_2|}. \quad (2.12)$$

This value is effected by galvanic distortion.

2. Bahr's 3D/1D, which is a phase sensitive skew:

$$\mu = \frac{\sqrt{|Im(S_2 D_1^*) + Im(D_2 S_1^*)|}}{|D_2|} \quad (2.13)$$

* indicates the complex conjugate and

3. Bahr's 3D/2D regional skew:

$$\eta = \frac{\sqrt{|Im(S_2 D_1^*) - Im(D_2 S_1^*)|}}{|D_2|} \quad (2.14)$$

Conclusions about the underlying geometry are made by applying certain thresholds to these parameters. Values of Swift's skew and Bahr's 3D/1D above 0.1 indicate more complex dimensionality, whereas for Bahr's 3D/2D a threshold of 0.3 for the 2D approximation is recommended. A comprehensive overview of dimensionality classification schemes can be found in Lahti et al. (2005).

2.3.1 Distortion model and strike analysis

Following the approach of Zhang et al. (1987), for measured impedance data (Z) only a distortion of the electric field is considered when estimating a geoelectric strike for a 2D regional structure with local 3D inhomogeneities:

$$Z = (I + P_h)Z^0. \quad (2.15)$$

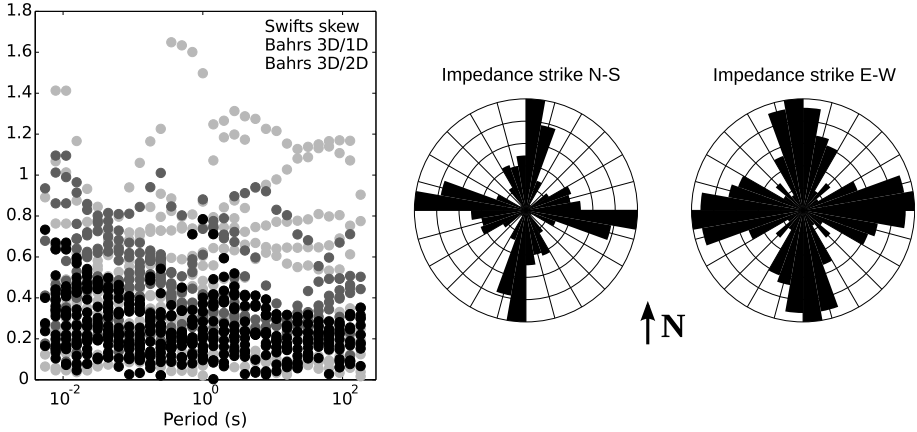


Figure 2.3. Rotational invariants and strike angles from García Juanatey et al. (2011). The difference in Swift's skew and Bahr's skew indicate galvanic distortion of the data.

Z_0 is the undistorted regional impedance, I the identity matrix and P_h is the distortion matrix, a real valued and frequency independent expression for the effect of galvanic distortion. To find the 2D regional strike direction one has to find an estimate of the angle θ_r from

$$Z(\theta_r) = \begin{bmatrix} P_{xy}Z_{yx}^0 & (1 + P_{xx}Z_{xy}^0) \\ (1 + P_{yy}Z_{yx}^0) & P_{yx}Z_{xy}^0 \end{bmatrix}. \quad (2.16)$$

For a 2D regional model, the diagonal components of the impedance tensor are related to the off-diagonal impedance elements in the same column as:

$$Z_{xx}(\theta_r) = \beta Z_{yx}(\theta_r) \quad (2.17)$$

$$Z_{yy}(\theta_r) = \gamma Z_{xy}(\theta_r). \quad (2.18)$$

with the static shift parameters β and γ that are frequency independent and can be calculated for each site with a least squares approach. Then one can estimate the best regional strike θ_r angle by minimizing the objective function Q (Smirnov and Pedersen, 2009) between measured and predicted off-diagonal impedance elements for $N = N_p N_S$ (number of periods times number of stations) data points by varying the strike angle θ :

$$\begin{aligned} Q(\theta) &= \frac{1}{4N - 2N_p - 1} \\ &\times \sum_i \sum_j \left(\frac{1}{\sigma_{xx_{ij}}^2} |Z_{xx_{ij}}(\theta) - \beta_i Z_{yx_{ij}}(\theta)|^2 \right. \\ &\left. + \frac{1}{\sigma_{yy_{ij}}^2} |Z_{yy_{ij}}(\theta) - \gamma_i Z_{xy_{ij}}(\theta)|^2 \right), \end{aligned} \quad (2.19)$$

and by considering the estimated variances σ of the diagonal impedance elements or an error floor, that is calculated as a percentage of the off-diagonal impedances. The parameters β and γ give some insights into the influence of static shift. However, it is not possible to fully recover P_h . A \sqrt{Q} -analysis can be conducted for several θ to estimate how far the data can support a certain strike direction over a profile of MT stations. The strike angles found with the described mathematical strategies have a 90° ambiguity and have to be supported by either a maximum phase criteria, VMT data or independent information, e.g. geological observations.

With real data from complex geological settings, it is often not possible to perform an unambiguous decomposition into E- and B-polarization, since the real structure is 3D and one cannot estimate a unique or even a well-defined strike direction for all frequency and sites. Pedersen and Engels (2005) showed that applying 2D inversion on the effective impedance or Berdichesvky determinant:

$$Z_{Det} = \sqrt{Z_{xx}Z_{yy} - Z_{xy}Z_{yx}} \quad (2.20)$$

which is a rotational invariant of the impedance tensor, is more robust in a 3D environment than E- or B-polarization.

In papers I and II, we always used the determinant of the impedance tensor. Nevertheless, a strike analysis has to be performed in order to project station locations and model sections accordingly onto a straight line perpendicular to the assumed strike direction.

2.3.2 Static shift corrections

In 2D, the most simplified description of galvanic distortion is a static shift on the apparent resistivity curves only. There are several approaches to overcome the effect of static shifts in MT:

1. Using information from other geophysical methods such as TEM (Transient electromagnetics), e.g. Pellerin and Hohmann (1990), to correct the data manually with overlapping transfer functions.
2. Statistical approximations that static shifts should sum up to zero along an expanded profile due to their Gaussian distribution or defining/finding an undistorted reference site. Spatial filtering of the electric fields along the profile (Singer, 1992) can be applied.
3. If available, long period data ($T > 10^4$ s) can be inverted for a one dimensional structure of the earth. The corresponding response data can be fitted to the measured data to derive a static shift correction (Zhdanov et al., 2010).
4. Down-weight the affected data (apparent resistivity curves of the E-polarization or determinant) and let the inversion take care of it by introducing small shallow features, or even to invert for the distortion matrix.

In 2D, there is the danger of over-fitting these extra parameters with a loss of structural information in the resistivity model.

In 3D, charge accumulations can be simulated by lateral conductivity changes in the near surface layers, therefore the discretization in the horizontal directions should be sufficiently fine. That might be a challenge in 3D due to the computational costs. The safest approach would be to also invert for the full distortion tensor (*A. Avdeeva, 2011, personal communication*). To investigate the effects of static shifts in 3D in a simplified approach, I calculated the impedance response for a simple 3D model (same as in paper II, see Fig. 2.4) using WSINV3DMT (description below). These synthetic data were then distorted with 5% Gaussian noise (on the absolute value of the main impedance) and a random static shift (P_{xx} and P_{yy} with a standard deviation of 0.5 and $P_{xy} = P_{yx} = 0$, so that only the apparent resistivity curves are effected). This data was then used for a three dimensional inversion with the true model as the prior model. As suspected, the inversion tried to fit the data close to the prior model and compensate the static shift with some conductive cells close to the station locations. The effect on the apparent resistivity data of one heavily distorted site is illustrated in Fig. 2.4c. Since the 3D inversion tries to fit all data (real and imaginary part of impedance) equally, also the modeled phase data is distorted to some degree. I draw the conclusion that even moderate to heavy static shift effects can be compensated for in 3D inversion with a sufficient discretization and enough degrees of freedom (free cells around the station locations). It is necessary to be cautious with the interpretation of small scale anomalies, but more regional parts of the model are not affected.

2.3.3 VMTs in 2D and 3D

Due to the boundary conditions, for the plane wave assumption, there is no vertical magnetic field for a 1D layered conductivity distribution. In the presence of lateral conductivity contrasts, a vertical magnetic transfer function can be estimated. It is usually displayed as induction arrows (Wiese, 1962), whose real part points away from good conductive features; their length provide an estimate for the strength and distance of the lateral resistivity contrast (e.g. Fig. 2.5). The direction of the induction arrows is another indicator for the geoelectrical strike direction. In 2D, only the component of the VMT that is perpendicular to the strike direction (or parallel to the profile) can be taken into account for inversion and interpretation, thus projecting possible off-profile conductors onto the 2D model. The VMT is also not affected by galvanic distortion (due to it being pure TE mode, see Becken and Pedersen (2003)).

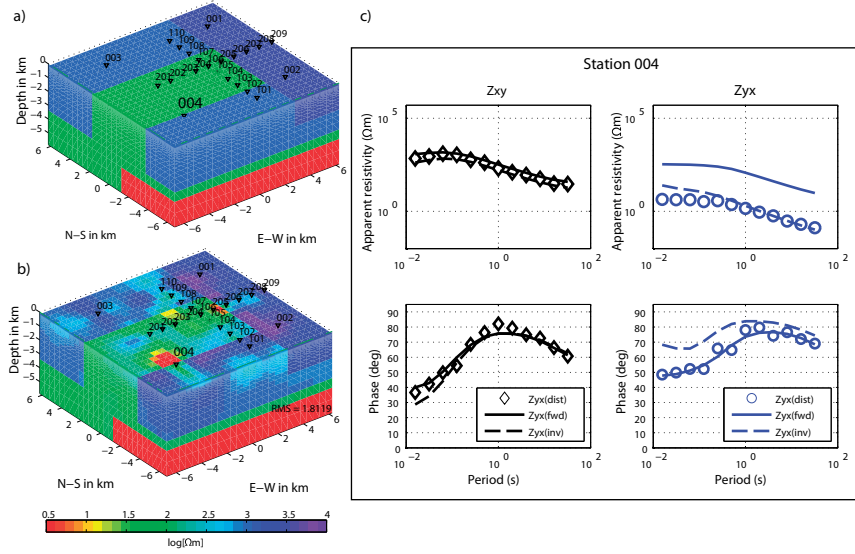


Figure 2.4. A synthetic study of static shifts in 3D inversion: a) synthetic model from paper II, b) inversion model using distorted data with an RMS of 1.8, both at 150 m depth. Especially around stations 004 and 205 there are ghost structures that are probably related to the imposed static shift. c) Apparent resistivity and phase data for the heavily distorted site 004, displayed are the true synthetic forward response (solid line), the distorted input data for the inversion (diamonds and circles) and the model response of the inversion (dashed line).

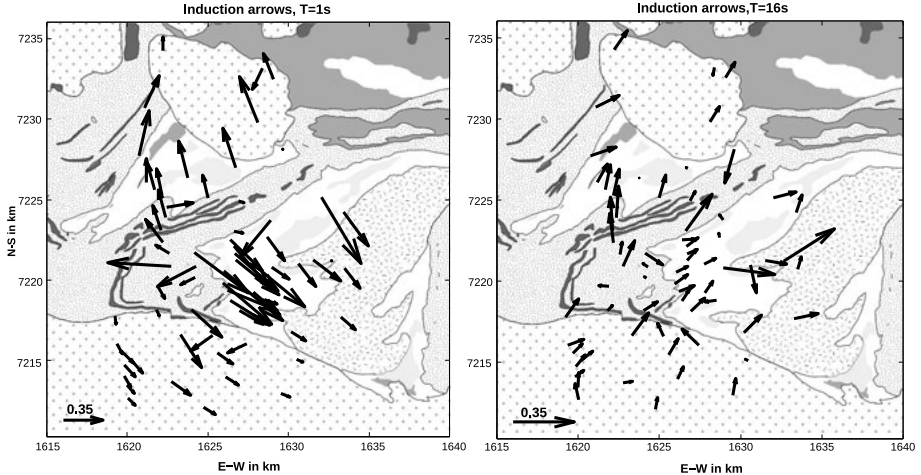


Figure 2.5. Measured vertical magnetic transfer function for the Kristineberg array for two periods (1 s and 16 s). For the short periods (left), they indicate a shallow conductivity anomaly in the central part of the array, whereas for the longer periods (right) a general trend towards the north-east is indicating a conductor to the south-west at greater depths

3. Inversion and forward modeling of MT data

The numerical approach to estimate and analyze a model (in this case the distribution of electrical resistivity within the Earth) from observed data (in our case the magnetotelluric impedance and vertical magnetic transfer function) is called *inversion*. The contrary procedure of computing synthetic data from a given parameter distribution is commonly referred to as *forward modeling*.

3.1 Forward modeling of EM fields

The forward modeling of electromagnetic fields for a given resistivity distribution requires a numerical solution of Maxwell's equations (see eq. 2.1 and 2.2). Currently, there are three main approaches (Avdeev, 2005): with finite differences (FD), finite elements (FE) and with the integral equation (IE) method. These approaches differ in the discretization of the model space and the numerical solution strategy.

In the *finite difference approach*, which is the base for the inversion algorithms used in this work, Maxwell's equations are solved by approximating the derivatives with the difference between neighboring points $x_{i+\frac{1}{2}} = x_i + \frac{dx}{2}$ in a rectangular staggered grid, usually in a so called *yee cell*.

$$\frac{f(x+dx) - f(x)}{dx} = f'(x + \frac{dx}{2} + O(dx^2)) \quad (3.1)$$

is the first derivative for a one-dimensional problem with errors in the order of $O(dx^2)$ (Bondeson et al., 2005). The main advantage is the relatively simple setup of the model. Difficulties arise for complicated geometries and topography.

The *finite element method* makes use of unstructured grids (meshes) with cubes, prisms or tetrahedrons as smallest elements. Maxwell's equations are solved using basis and weighting functions. The computational complexity is rewarded with the ability of mesh adaption and the inclusion of topography.

Thirdly, the *integral equation approach* (or method of moments) defines a scattering problem using the integral form of Maxwell's equations. The Green's function method is applied for a volume V^S with a different conductivity than the layered surrounding to solve for the unknown electric field E and a conductivity distribution σ :

$$E(r) = E_0(r) + \int_{V^S} G_0(r, r')(\sigma - \sigma_0)E(r')dr', \quad (3.2)$$

where G_0 is the electric dyadic Green's function for the layered background with conductivities σ_0 , and the free term E_0 is known. Only the anomaly (or scatterer) in the model is discretized, but the setup of the appropriate Green's functions and equations is fairly complicated. The code *x3d* by Avdeev et al. (2002) that was used to compute the forward VMT response in paper III is based on this approach. It allows for the computation of the EM fields for a scattering problem in a layered earth for the natural plane-wave field or controlled sources.

All three approaches result in a linear system of equations with the boundary conditions b and the sought-after field components x :

$$A \cdot x = b \quad (3.3)$$

that can be solved according to the nature of A . For 3D modeling, A can be very large, and the solution of this system accordingly unfeasible with direct methods. Therefore, nowadays often iterative methods and preconditioners are used (Avdeev, 2005; Boerner et al., 2008).

Forward modeling is an essential part of inversion algorithms. As an independent procedure, it is exceptionally useful in all stages of 1D, 2D and 3D strategies to evaluate strengths and weaknesses of inversion and interpretation by testing many kinds of hypotheses for data and models.

3.2 Inversion of MT data

In the determination of the Earth's structure from geophysical measurements, mathematical inversion methods have always played a key role (Menke, 1984). They comprise techniques that derive a model vector m of a certain parameter from a set of N measured data d . The general mathematical formulation for an inverse problem is:

$$d = F(m) \quad (3.4)$$

The solution to this problem depends heavily on the nature of the relation between data and model as well as the number of data points and model parameters. In electromagnetics as in other geophysical applications, this relation is usually not linear and the problem can be mixed or under-determined, i.e. the number of independent data points is much smaller than the number of model parameters for at least some parts of the problem. Since F , the kernel of the inverse problem, can not be inverted directly with a unique solution, it is common practice to minimize the difference between the measured data d^{obs} and the predicted data of a given model m^{est} :

$$\chi_d^2 = (d^{obs} - F(m^{est}))^T C_d^{-1} (d^{obs} - F(m^{est})). \quad (3.5)$$

C_d is the data covariance matrix, generally assumed to be only non-zero on the diagonal elements due to independent measurement errors. Due to the ill-posedness of the problem, the inversion may result in many, with respect to

data fit, equivalent models. To avoid structures that are actually not required by the data, the roughness of the model, as measured by the model norm χ_m is minimized towards prior information or a minimum-structure-constraint:

$$\chi_m^2 = (m - m_0)^T C_m^{-1} (m - m_0) \quad (3.6)$$

with m_0 as the prior model, C_m as the model covariance matrix, which can be replaced by a smoothness operator. So the actual objective functional to be minimized during the inversion process is a combination of equations 3.5 and 3.6:

$$\phi = \chi_d^2 + \lambda \chi_m^2 \quad (3.7)$$

with the trade-off parameter λ .

In the case of *joint inversion*, the objective function is extended to include multiple data sets.

3.2.1 2D and 3D MT inversion algorithms

Both REBOCC (Siripunvaraporn and Egbert, 2000) and WSINV3DMT (Siripunvaraporn et al., 2005) are inversion algorithms that use the principle of finite differences to discretize the model space with rectangular cells and follow Occam's inversion scheme to find a smooth model (Constable et al., 1987). Their advantage is the approach of performing the inversion in the (possibly even reduced) data space, which can downsize the problem to a computational load that is manageable on a desktop computer. Mathematically, this is accomplished by finding stationary points of the function:

$$\begin{aligned} U(m, \lambda) &= (m - m_0)^T C_m^{-1} (m - m_0) \\ &+ \lambda^{-1} ((d - F(m))^T C_d^{-1} (d - F(m)) - \chi_*^2), \end{aligned} \quad (3.8)$$

χ_*^2 is the desired misfit, that normally equals to N . λ , the so-called Lagrange multiplier, balances good data fit with smooth models. In each iteration of the inversion process, several λ are tested to minimize the data fit χ_d^2 towards the desired misfit level or to maximize λ to smooth the model, if the desired misfit level has been reached. Smooth inversion of MT data is meaningful, since also the EM fields are diffusive, even though resistivity changes in nature can be very sharp. Other, more "blocky" inversion strategies exist, but are not dealt with here.

To find the stationary points of equation 3.8, $W_\lambda(m)$ is minimized instead:

$$\begin{aligned} W_\lambda(m) &= (m - m_0)^T C_m^{-1} (m - m_0) \\ &+ \lambda^{-1} ((d - F(m))^T C_d^{-1} (d - F(m))), \end{aligned} \quad (3.9)$$

Due to the nonlinearity of the magnetotelluric problem, $F(m)$ has to be linearized with a Taylor series expansion and an iterative solution strategy is

applied:

$$F(m_{i+1}) = F(m_i + \delta m) = F(m_i) + J \cdot (m_{i+1} - m_i), \quad (3.10)$$

where $J_i = \partial F / \partial m_i$ is the $N \times M$ sensitivity matrix calculated at each iteration i that can be very computationally costly in 3D. The data space approach eventually iterates the solution with:

$$\begin{aligned} m_{i+1} - m_0 = & C_m J_i^T C_d^{-1/2} [\lambda I + C_d^{-1/2} J_i C_m J_i^T C_d^{-1/2}]^{-1} \\ & \times [d - F(m_i) + J_k(m_i - m_0)]. \end{aligned} \quad (3.11)$$

For each iteration, several values of λ are tested, each of which involves the computation of a forward response. The approach in data space by Siripunvaraporn and Egbert (2000) and Siripunvaraporn et al. (2005) is computationally advantageous, since in most practical applications, there are far fewer data points than model parameters. This is especially true in 3D.

Adding the third dimension to MT data inversion is a huge leap. The number of model parameters is several orders of magnitude larger. More data is required to actually cover a grid. Solving the inversion problem is computationally demanding, both regarding the number of equations to be solved as well as memory requirements for the storage of e.g. sensitivity matrix's. It is on the transition of only being feasible on multi-core computers, using parallelized routines, since the evolution of computational power goes into that direction rather than towards enhanced work stations (Newman et al., 2003; Siripunvaraporn and Egbert, 2009; Zhdanov et al., 2010). While for 2D inversion a large number of algorithms exists that are well tested and available in commercial and non-commercial software packages, 3D inversion is still in its adolescence. Available to the academic community is the single-processor version of WSINV3DMT by Siripunvaraporn et al. (2005), which can be applied to small to moderate sized models and data sets. All components of the impedance tensor with real and imaginary parts are inverted on a rectangular grid. A prior model has to be provided with the possibility to use a homogeneous half space for structure minimization. For real data applications it is therefore praxis that 2D models are tested rather rapidly for any kind of assumption (prior models, different data inclusion, different inversion parameters), whereas 3D inversion is carried out for a few and well considered cases due to the much longer computation time.

For the 2D inversion in paper I and II, REBOCC (Siripunvaraporn and Egbert, 2000) was used to invert for apparent resistivity and phase of the different components of the impedance tensor (TE, TM, DET) as well as VMTs on a rectangular grid. Different error floors can be applied, e.g. to down-weight apparent resistivities for static shift effects. Prior information can be built in as fixed model parts and boundaries in the regularization. In paper IV, the algorithm EMILIA (Kalscheuer et al., 2010) was applied on both synthetic and field data sets. It is an advancement of REBOCC with many new features, e.g.

joint inversion with geoelectric data and 1D inversion of controlled source data including static shift factors.

Model assessment

Due to the ill-posedness of the MT problem, inversion algorithms can only provide ambiguous results, i.e. a variety of models that equally fit the data. Therefore, a careful assessment of the derived model has to be performed to justify the selection of a preferred solution. There are several approaches to evaluate the sensitivity of model features, some of which can get very computationally demanding in 3D and are therefore time consuming to perform. Systematic forward modeling (Nolasco et al., 1998; Schwalenberg et al., 2002) has been used to study the sensitivity of certain features in the inversion models for paper I, II and III. In this approach, parts of the derived model are varied and the misfit between forward response and observed data is calculated. It is useful as an estimation of the resolution of certain parts of the model, but is actually only a linear analysis and therefore only valid for small model perturbations.

Model assessment can also be approached by comparing the inversion results from different data subsets, in 2D e.g. E- and B-polarization and determinant, or including the vertical magnetic transfer function. In 3D, it was not possible to invert for the VMT. Nevertheless, forward modeling of the VMTs from the resistivity model derived by impedance inversion alone and the comparison to the field data provided some validation of the selected model in paper III.

A systematic approach for sensitivity analysis in 3D has not been developed, and is heavily dependent on computation time.

3.3 MT in combination with other geophysical methods

Most geophysical surveys nowadays are conducted with more than one technique. On a crustal scale, especially the integrated interpretation with seismic data, e.g. reflectivity patterns, location of earthquakes or tomographic seismic velocity information has proven to be a very fruitful union (e.g. Jones, 1998). Although some joint inversion techniques are already applied, integrated interpretation is performed most commonly after single inversion of the individual data sets (*cf.* paper I and III). Joint inversion requires some bulk or structural correlation between electrical conductivity and seismic properties, that can be enigmatic and dependable on site conditions (Bedrosian, 2007). The joint inversion of MT and potential field data is the subject of recent investigations, e.g. Moorkamp et al. (2011).

In investigations of the shallow subsurface, other geophysical methods that probe the electrical resistivity as e.g. electrical resistivity tomography (ERT) are jointly applied together with RMT.

Reflection seismics

Changes in the acoustic impedance (the product of seismic wave velocity and density) of rocks give rise to reflectivity patterns in seismic recordings. A good estimate of seismic velocities is necessary to convert the arrival times in the seismogram to depth and to find the correct position of reflectors in the subsurface. Reflection seismic imaging is widely used in hydrocarbon exploration as well as in studies of the crust and mantle (e.g. Juhlin et al., 2002). Its resolution is superior to any other geophysical method and can be controlled by the acquisition parameters (frequency, layout, choice of source). Due to its popularity, advances in the processing and interpretation of complicated geometries are constantly undertaken. However, crustal studies are not yet easily conducted in 3D, most surveys are restricted to, sometimes crooked, profile lines. Only for promising exploration targets the effort of 3D data acquisition is undertaken. Seismic signal processing is rather sophisticated. MT data are mainly sensitive to conductors and provide less spatial resolution for deeper structures, depending heavily on the conductivity of overlying layers. Lateral resolution is better and comparable to that of reflection seismics due to the mainly horizontally flowing currents caused by the plane wave incidence.

Joint interpretation can also include the use of prior models derived from another method. In paper II, known seismic reflectors were introduced into the inversion as possible resistivity boundaries, allowing for less smoothing across them in the inversion process. With this approach, the data fit of the MT data could even be improved.

Direct current resistivity

Direct current resistivity methods, also called electrical resistivity tomography (ERT), is also imaging the resistivity distribution of the shallower subsurface by injecting currents with two steel electrodes and recording the arising potential difference at two voltage electrodes (Ernstson and Kirsch, 2006). During the last decades with the development of fast and reliable instruments like the multi-electrode array (Dahlin and Zhou, 2006), it has become very popular to utilize ERT for a great variety of near-surface applications. Commercial software packages to invert 2D and 3D data sets like RES2DINV and its three-dimensional counterpart RES3DINV (Loke and Barker, 1996) are widely used even by non-geophysicists. Joint inversion can benefit from the different sensitivities of both methods that sense the same resistivity distribution. Kalscheuer et al. (2010) illustrated with a smoothness-constrained linearized analysis how ERT has good resolution of both resistive and conductive features, but lacks the penetration depth of the RMT method, which in turn can best resolve conductive features. For the joint approach, it is necessary to apply different weighting on the included data sets to account for different amounts of data points, different sensitivities of the methods and equally well fit all data with a model that benefits from both methods.

4. Introduction to the field areas

The case studies contained in this thesis represent very different geological settings. Paper I, II and III contribute to a regional study of the structure of the upper crust in the Kristineberg area, Skellefte district in northern Sweden, using broad band magnetotelluric data. The model scale is several kilometer. As a contrast, paper IV describes the investigations of the shallow subsurface down to 60 m to monitor the groundwater contamination after a well blow-out close to the town Trecate, Italy, with radiomagnetotelluric measurements.

4.1 Kristineberg, western Skellefte district, northern Sweden

The Kristineberg area is part of the western Skellefte district (Årebäck et al., 2005; Skyttä et al., 2010) and has for the last years been studied intensively with geological and geophysical methods. The Skellefte District (see Fig. 4.1) in northern Sweden is known for its abundances in volcanic hosted massive sulfides (VHMS) mineral occurrences. It constitutes part of the Svecofennian province (ca. 1.90 to 1.8 Ga) and lies at the boundary between the domain of supracrustal rocks with recycled Archean rocks (Gaal and Gorbatshev, 1987; Weihs et al., 1992; Rutland et al., 2001) to the north and the high-grade metamorphic (amphibolite facies) rocks of the Bothnian basin to the south. The latter consists largely of greywackes, gneisses and migmatites (Weihs et al., 1992; Bergström, 2001). The supracrustal rocks in the western part

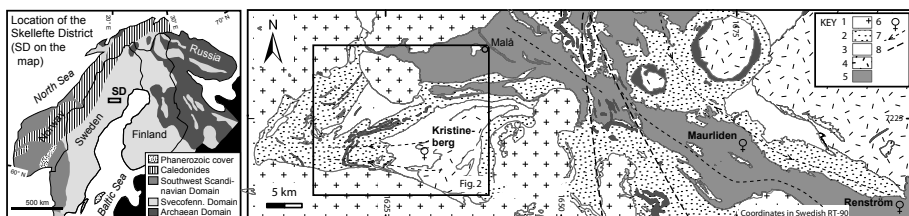


Figure 4.1. Location of the Skellefte district, northern Sweden. Key: Left: Geological overview of the Fennoscandian Shield. Right: Geological sketch of the western part of the Skellefte District. 1) Late- to post-tectonic granites 2) Metasediments 3) Skellefte Group metavolcanic rocks 4) Mafic intrusions 5) Metagranitoids 6) Active mines 7) Axial trace of the main folds 8) Post-main deformation shear zones. Geology reproduced with kind permission from the Geological Survey of Sweden.

of the Skellefte district comprise a sequence dominated by subaqueous volcanic rocks (the Skellefte group) and a sequence dominated by shallow-water to subaerial sedimentary (the Vargfors group, Allen et al. (1996); Bauer et al. (2011)) and intrusive rocks (Revsum granite, 1.82 – 1.78 Ga, and Viterliden intrusion, ~ 1.85 Ga, Skyttä et al. (2011)). The origin of the basement is in debate (Tryggvason et al., 2006).

Due to a limited number of outcrops, the surface geology is mainly defined with the support of airborne geophysical data. In the Kristineberg area (Årebäck et al., 2005; Skyttä et al., 2010), the main lithological units are metamorphic rocks of the Skellefte and Vargfors groups forming an anticline that is plunging to the west, cored by the Viterliden intrusion to the east and constrained by the intrusive rocks of the Revsum granite to the south, west and north, with an estimated maximum depth extent of about 3 - 4 km (Malehmir et al., 2009).

The area has been intensively investigated during recent years: A pilot study of geophysical investigations was launched in 2003, including potential field modeling and two reflection seismic profiles (Tryggvason et al., 2006; Malehmir et al., 2007) resulting in a pilot 3D geological model presented by Malehmir et al. (2009) which included 3D inverse gravity modeling and reflection seismic studies.

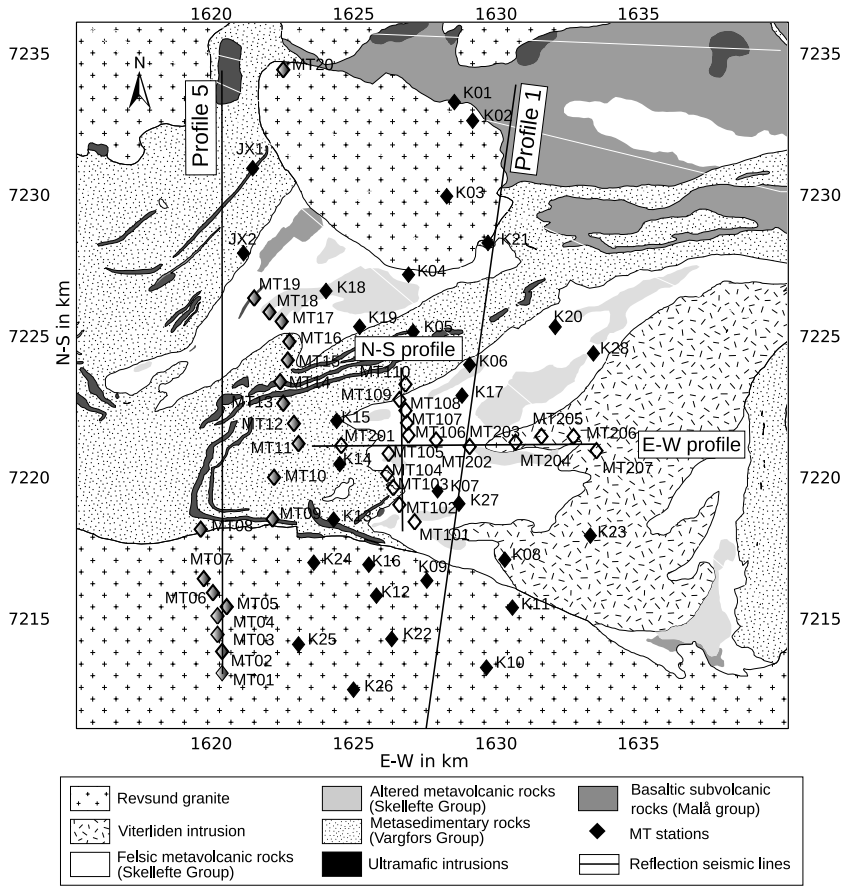


Figure 4.2. Geologic map of the study area with the position of MT sites and the previous seismic profile. Different shadings for the MT sites indicate different field campaigns.

4.2 Trecate site, Italy

The survey area is a part of the aquifer at Trecate in the Piemonte region of Italy (see Figure 4.3). In 1994 the site was the scene of an inland crude oil spill following an oil well blow-out from an ENI-Agip operated exploration well Cassiani et al. (2004). The incident resulted in approximately 15,000 m³ of middleweight crude oil being released overland contaminating both soil and groundwater. Immediately after the blowout, a control network of piezometers to monitor the groundwater was established. The geophysical data were acquired in the framework of the SoilCAM project in Trecate area close to the city of Milan, Italy (for more information see: www.soilcam.eu) to monitor the development of remediation.

The geological setting is determined by the Po river aquifer which at Trecate comprises an extensive, unconfined sand and gravel unit in excess of 60 m thickness beneath the site. The site stratigraphy is characterized by a thick sequence of poorly sorted silty sands and gravels in extensive lenses, typical of braided river sediments. An artificial layer of clayey-silty material, less than one meter thick and originally laid in place as a liner for the rice paddies, overlies most of the site. The area is characterized by alluvium, fluvio-glacial and fluvial, whose hydrogeological properties are due to the texture-sedimentology aspects, to the age and to the alteration degree. The location of the geophysical measurements is in an agricultural area (Figure 4.3), with corn fields and rice paddies. The groundwater level at the site has a seasonal fluctuation of 6 m, with higher levels occurring during the summer period because of the surface recharge from the agricultural irrigation practices.

Even after the remediation processes were carried out, a considerable amount of contaminants has been detected in the groundwater samples taken in the area. The remaining hydrocarbons form a thin film on top of the groundwater surface. Due to the seasonal variation of the water level and higher viscosity of the hydrocarbon, it migrates slower than the water in the porous media above the lowered groundwater surface and forms a zone so-called “smearing zone”.

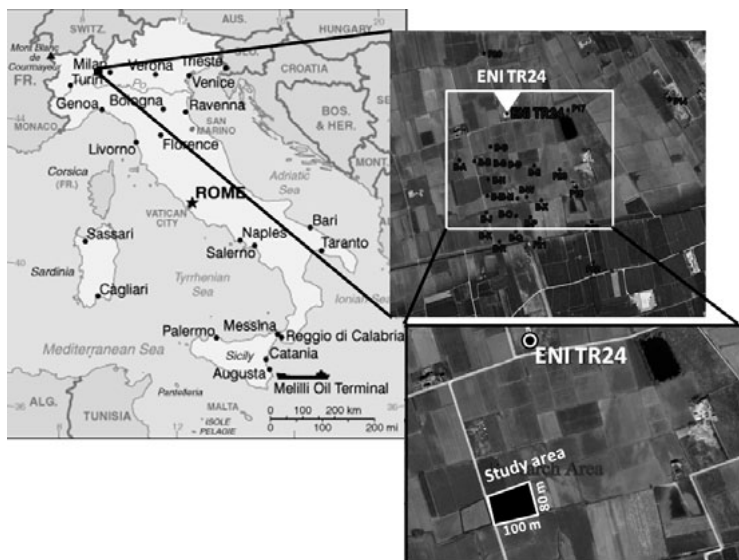


Figure 4.3. Location of the study area in Italy. ENI TR24 is the blown-up oil well.

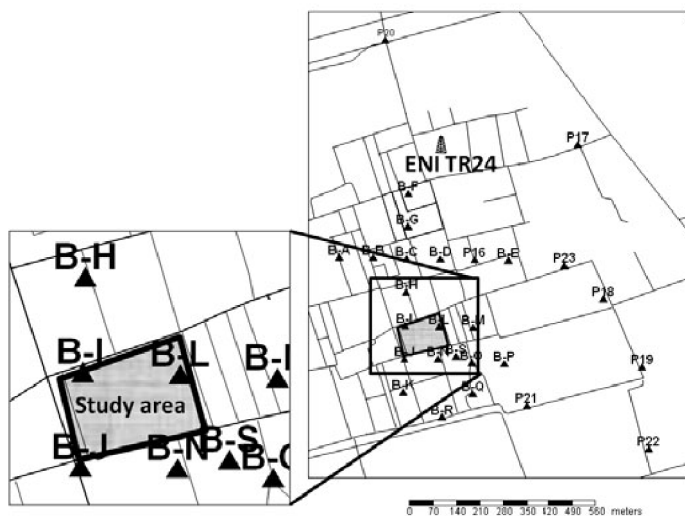


Figure 4.4. Location of piezometric boreholes for groundwater monitoring in the Treccate area.

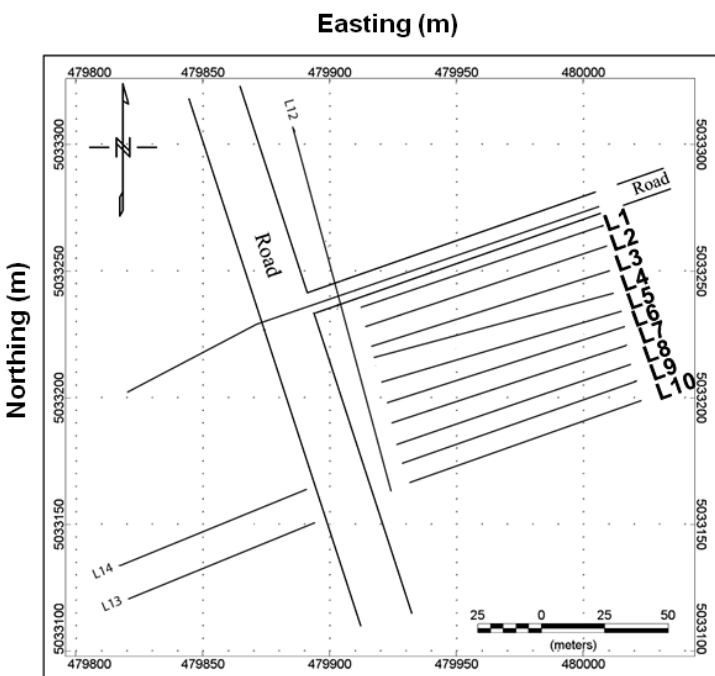


Figure 4.5. Location of the ERT and RMT lines (L1-L10) measured at the Trecate site.

5. Summary of papers

5.1 MT measurements in the western part of the Paleoproterozoic Skellefte Ore District, Northern Sweden: A contribution to an integrated geophysical study.

A 2D conductivity model of the Kristineberg area in the Skellefte Ore District, Northern Sweden, was derived from magnetotelluric measurements. In this pilot study, 20 broadband MT stations were installed along a 20 km long north-south profile (Profile 5 in Fig. 4.2). Data quality was good and single site processing was sufficient to obtain stable transfer functions in the range of 700 Hz to 700 s with the processing software by Smirnov (2003). Dimensionality analysis after Zhang et al. (1987) shows that a 2D interpretation of the data is justified, although the presumed geoelectric strike direction of N75°E is not consistent over the whole profile.

The determinant of the impedance tensor was inverted for a 2D model with the algorithm REBOCC by Siripunvaraporn and Egbert (2000) as modified by Pedersen and Engels (2005), applying an error floor of 90% for apparent resistivities (in order to down weight for static shift effects) and 2.8° for phases (corresponding to 5% on impedances). The derived model could fit the data to an RMS of 1 and depicts strong contrasts in electrical resistivity along the profile. The new conductivity model of the upper crust has good correlations to the results from the seismic studies and allows for a geological interpretation of the model features (letters refer to Fig. 5.1):

1. Sedimentary basin, reflective and conductive (CI).
2. Revsund-Granites, crystalline, reflective and resistive (RI).
3. Metasediments with mafic intrusions, resistive and reflective (RII-IV).
4. Skellefte Volcanics, conductive and not reflective (CII).
5. Dense intrusion/mineralization, conductive and seismically diffractive (CIII).

Interpreting both independent data sets confirms the major features from the previous model (Malehmir et al., 2009), such as the thickness of the Revsund granites in the south, the existence of a structural basement with metasedimentary origin, and gives new insight into the nature of the volcanic rocks and their possible mineral content.

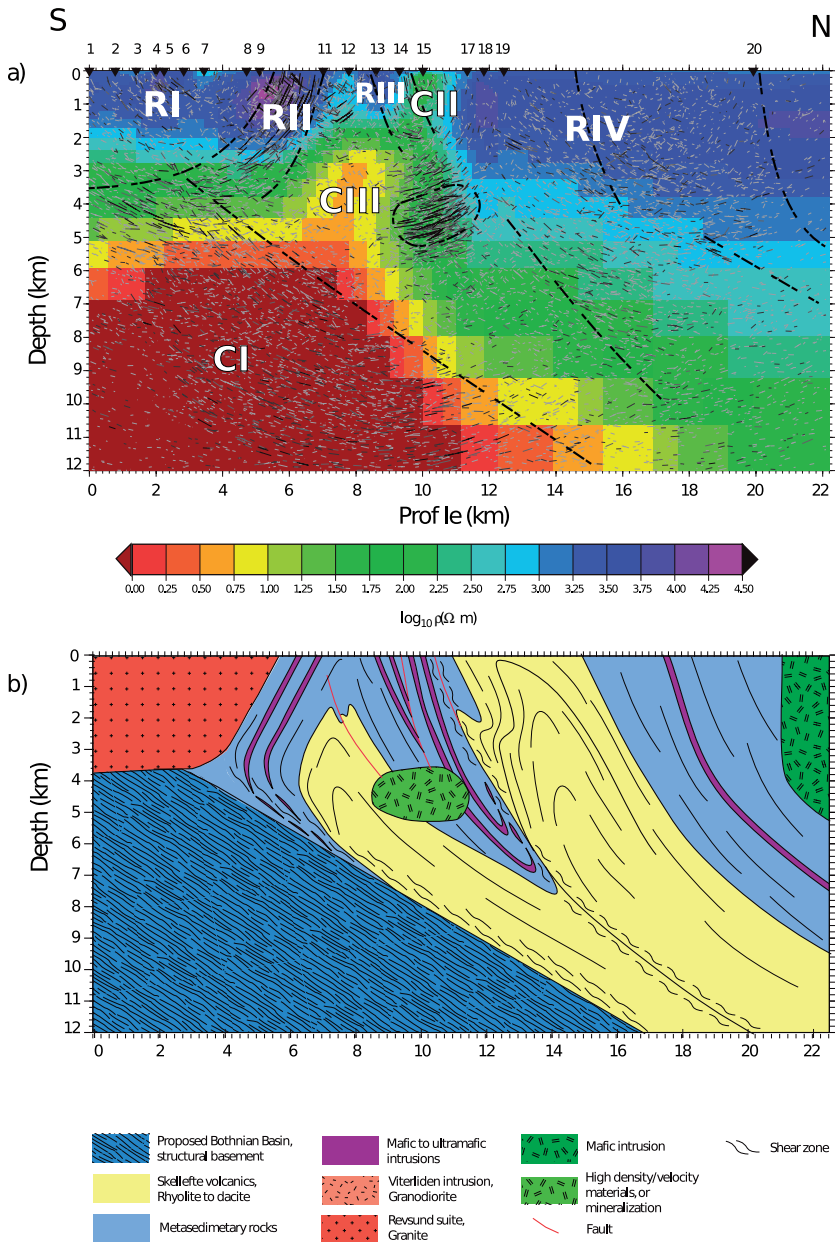


Figure 5.1. Comparison of a) MT inversion model with seismic reflections from Tryggvason et al. (2006) and b) geologic cross section that concluded information from seismic reflection, potential field modeling and field observations from Malehmir et al. (2007).

5.2 Imaging the Kristineberg mining area with two perpendicular magnetotelluric profiles in the Skellefte Ore District, northern Sweden.

Magnetotelluric (MT) data from two perpendicular profiles in the Kristineberg area (labeled N-S-profile and E-W profile in Fig. 4.2), northern Sweden, have been analyzed and modeled. Seventeen broadband magnetotelluric stations were installed along two existing seismic reflection lines close to the Kristineberg mine. The profiles were 6 and 12 km long with 500 m and 1 km site spacing, respectively. The obtained MT transfer functions, again using the algorithm by Smirnov (2003), are in the period range of 0.0015-200 s and of fairly good quality. A detailed strike and dimensionality analysis was performed, using the approaches by Zhang et al. (1987) and Bahr (1991). It reveals consistent, but period dependent strike directions, indicating a change in the geoelectrical strike with depth. Therefore, the determinant of the impedance tensor was used to derive 2D inversion models along both profiles. Using the algorithm REBOCC by Siripunvaraporn and Egbert (2000) and applying again an error floor of 90% for apparent resistivities and 2.8° for phases additionally to the measurement errors, two stable conductivity models with good data fit were obtained. The addition of seismic reflection information from the co-located survey (Dehghannejad et al., 2010) as a priori information in the inversion, further improved the data fit on the N-S profile. Extensive sensitivity analyses following the approaches by Nolasco et al. (1998); Park and Mackie (2000); Schwalenberg et al. (2002) helped to delineate the well resolved regions of the models and to determine the position of pronounced boundaries.

To further study the influence of 3D effects on 2D inversion models of the determinant, a 3D synthetic test was performed. A representative 3D conductivity model was constructed considering the geometry of the actual field setup (see Fig. 5.2). Using WSINV3DMT by Siripunvaraporn et al. (2005), the 3D forward response of this model was calculated and 5% Gaussian noise was added unto the impedance elements. Then 2D inversion models using the determinant of the impedance tensor along the two perpendicular profiles were derived and compared to the true synthetic model. With the insights from this study we can identify possible artefacts introduced by the 2D inversion:

1. Shallow conductors will be smeared downwards and their depth extent cannot be resolved.
2. The depth of resistors might be shallower than in the true model.
3. The depth to the top of the deep conductor is too shallow.
4. A southern off-profile deep conductor would have a significant influence on the E-W model.

In the two final models (see Fig. 5.3), the geoelectrical features can be associated with lithological units. The conductor CII is probably related to the shallow graphitic shales in the contact between the Skellefte and Vargfors groups. The rocks of the Skellefte group are imaged by RI, RIII and RVI. By projecting

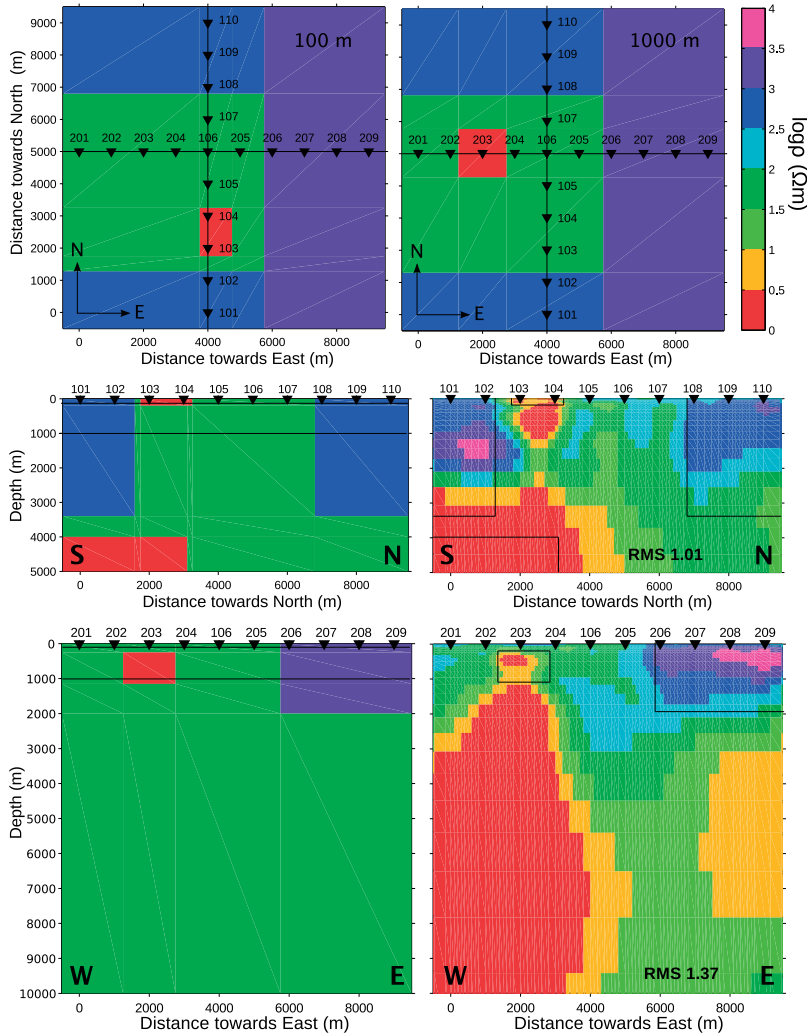


Figure 5.2. A 3D synthetic model and the 2D inversion of the forward responses. At the top two depth slices at 100 and 1000 m respectively, showing the location of the stations and the profiles. Below, vertical slices along the profiles through the synthetic model (left) and the resulting model from the 2D inversion of the synthetic data (right). The overlying black lines correspond to the true location of the model features.

the known 3D geometry and position of the ore lenses from the nearby mines (Rävldiden, Rävlidmyran and Kristineberg) on top of the resistivity models as shown in Fig. 5.3, it is possible to see a good correlation with conductors CIII, CIV and CV from both profiles. This might indicate that these conductors are caused by the hydrothermally altered rocks of the ore horizons. The Viterliden intrusion is probably related to the resistor RII. Finally, the deep

conductor CI, interpreted as the structural basement of metasedimentary rocks of the Bothnian Basin, is present in both profiles, with an estimated depth of 5-7 km.

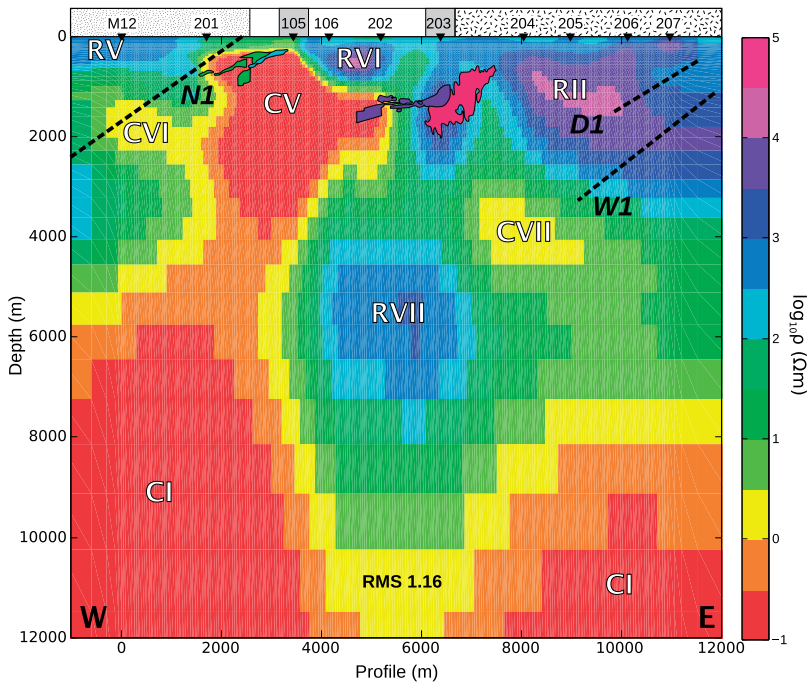
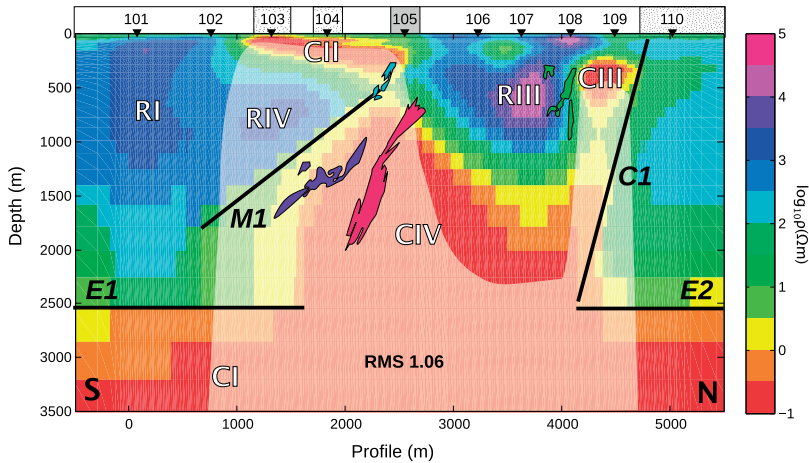


Figure 5.3. 2D inversion model for N-S and E-W profiles. Site positions are marked as black triangles, geology along the profile (key is as in Figure 4.2). Black lines represent modeled reflections (after Dehghannejad et al., 2010), solid lines are the ones included in the MT inversion, dashed lines were not. Colored regions enclosed in black lines are the projection of the 3D geometry of the ore bodies. White fading indicates poorly resolved features. Ore body geometries are reproduced with the permission from Boliden Mineral AB.

5.3 Upper crustal resistivity structure of the Kristineberg area, Skellefte district, northern Sweden revealed by 3D magnetotellurics.

In addition to the data collected for paper I and II, further MT measurements were carried out in the Kristineberg area to construct a three-dimensional model of the crustal electrical resistivity. The impedance tensor was again derived using the time series processing of Smirnov (2003). From the total number of 67 sites, 42 with the best data quality were selected for 3D inversion with the algorithm WSINV3DMT by Siripunvaraporn et al. (2005), using 12 periods and applying an error floor of 10% onto the impedance elements. The chosen model has a RMS of 3.3, but represents the geoelectrical structure reasonably well.

Forward modeling of vertical magnetic transfer function data with the integral equation approach by Avdeev et al. (2002) supports the model which was derived from the magnetotelluric impedance only. The dominant features in the 3D model (see Fig. 5.4) are the strong conductors at various depth levels and resistive bodies of variable thickness occurring in the shallower subsurface. The deepest conductor (CI in Fig. 5.4), previously identified as the Skellefte crustal conductivity anomaly, is imaged in the southern part of the area as a north-dipping feature starting at ~ 4 m depth. Several shallow conductors (CII) are attributed to graphitic black shales defining the contact between the metasedimentary rocks and the underlying metavolcanic rocks. Furthermore, an elongated intermediate depth conductor (CIII) is possibly associated with alteration zones in the metavolcanic rocks that host the ore occurrences. The most prominent crustal resistors occur in the southern and northern part of the area (RIa and RIb), where their lateral extent on the surface coincides with the late-orogenic Revsund type intrusions. To the east, a resistive feature (RII) can be correlated to the early-orogenic Viterliden intrusion.

The 3D model is compared with two previous 2D inversion models along the two perpendicular profile from paper II (N-S profile in Fig. 5.5 and E-W profile in Fig. 5.6). The main electrical features are confirmed with the new model and previous uncertainties regarding 3D effects, caused by off-profile conductors, can be better assessed in 3D, although the resolution is lower due to a coarser model discretization. The comparison with seismic sections along two north-south profiles reveal good correspondence between electrical features, zones of different reflectivity and geological units.

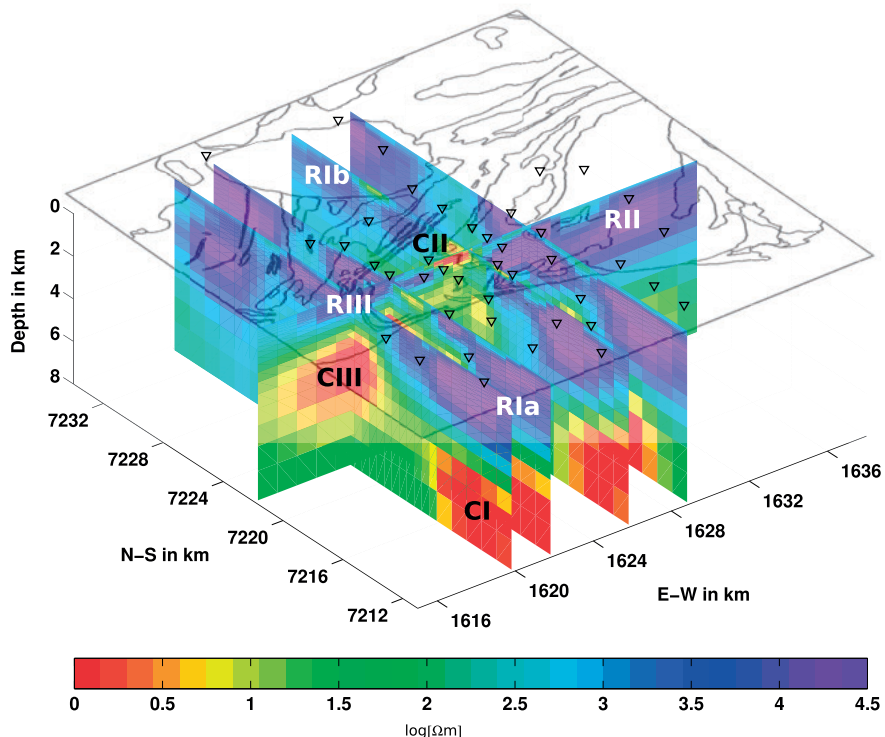


Figure 5.4. Slices through the 3D conductivity model of the Kristineberg area with overlying geologic map. Features: RIIa+b - Revsund granite, RII - Viterliden intrusion, RIII - Mafic dykes within metasediments, CI - Skellefte crustal anomaly, CII- shale-bearing metasediments, CIII- alteration zones within the volcanic rocks.

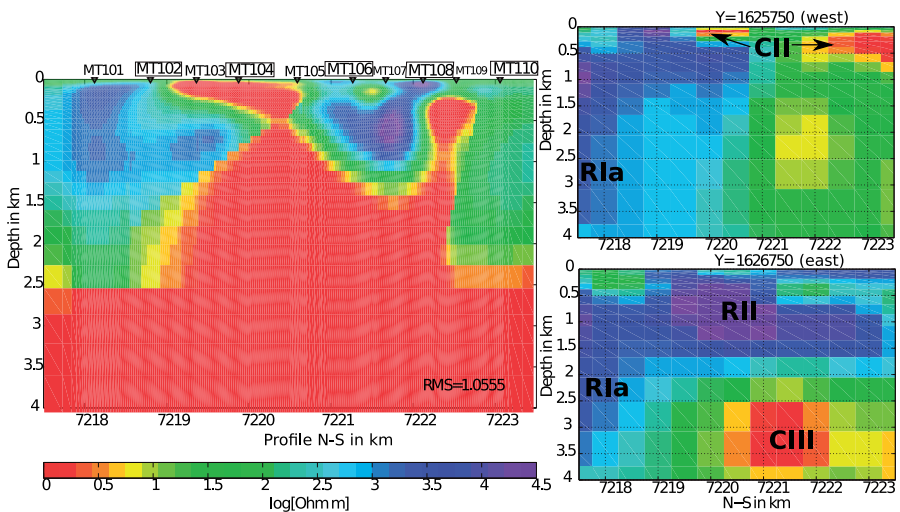


Figure 5.5. Comparison between 2D (left) and 3D (right) inversion models along the N-S profile. Due to the strong lateral changes, it is necessary to show two slices through the 3D model, 1 km apart. Boxed station names indicate sites included in the 3D inversion.

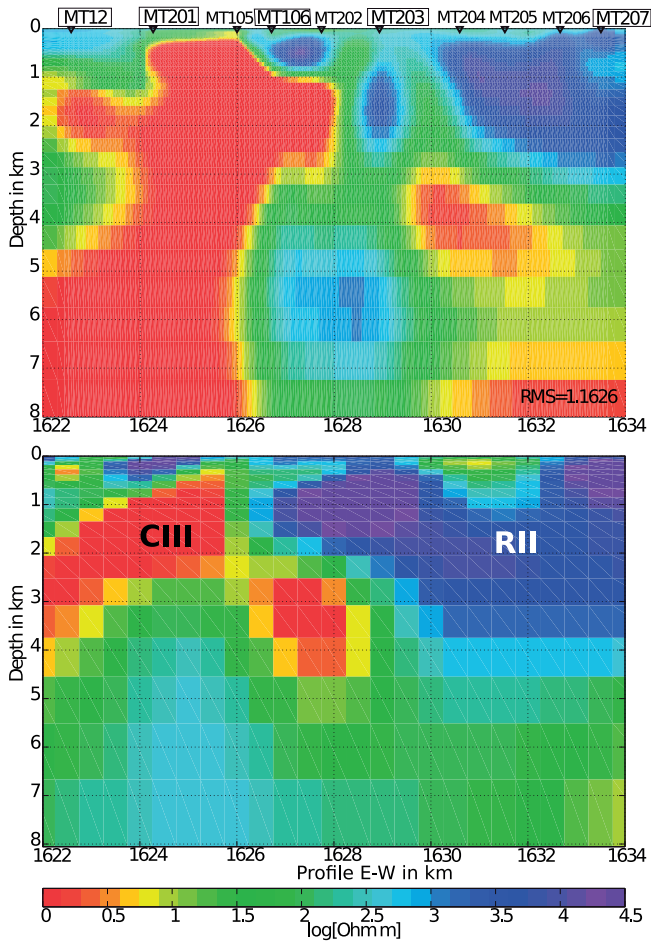


Figure 5.6. Comparison between 2D (upper) and 3D (lower) inversion models along the E-W profile. Boxed station names indicate sites included in the 3D inversion.

5.4 2D joint inversion of RMT and ERT data versus individual 3D inversion of full tensor RMT data. An example from the Trecate site in Italy.

Tensor Radiomagnetotelluric (RMT) and Electrical Resistivity Tomography (ERT) measurements have been carried out along ten parallel lines to image the electrical resistivity of the vadose and the saturated zone located below an area near the town of Trecate, 45 km west of Milan in Italy (Figure 4.3). In 1994, the area was exposed to an oil contamination caused by a tank explosion and has since been subject to monitoring and remediation programs. Our investigations are part of the SoilCAM project. Due to densely sampled RMT data, that was collected with the EnviroMT instrument (Bastani and Pedersen, 2001; Pedersen et al., 2006), it was possible to perform a 3D inversion of full tensor RMT data using the algorithm by Siripunvaraporn et al. (2005). The 3D model imaging the electrical conductivity was compared with the results from 2D joint inversion of RMT impedance determinant and ERT data along the single profiles, that was conducted with the approach by Kalscheuer et al. (2010). Firstly, a synthetic 3D resistivity model with resistivity variations close to those measured at the Trecate site was generated to compare resistivity models from a 2D joint inversion of determinant RMT and ERT data with those from 3D inversion of full tensor RMT data. In the joint inversion approach it is necessary to weight the different data sets to derive a model that fits both data sets equally. This is due to the number of data employed from different methods, the sensitivities of the different methods the non-linear nature of the corresponding forward problems. In this investigation, RMT data was five times more weighted than ERT data. The results from the synthetic modeling reveals that electrical resistivity models derived from 2D joint inversion of ERT and RMT data show more details of resistivity variations closer to the surface compared to the resistivity models from the 3D inversion of tensor RMT data. High resistivity structures are better resolved in the 2D joint inversion models while the more conductive features are better recovered by the 3D inversion. Furthermore, the model from 3D inversion of RMT data has a generally higher accuracy to estimate the depth to the top of conductor. Both methods suffer from decreasing resolution with depth. We deduce that it might be difficult to resolve the thin smearing zone caused by the oil contamination above the aquifer.

Applying the same approaches, the ERT and RMT data collected in the Trecate site were analyzed. Using the measured tensor RMT data it was possible to carry out full 3D inversion to study the details of underlying geology. The presented 3D inversion model (see Fig. 5.8) has an RMS fit of 1.5 in respect to the used error floor of 5% on the main impedances. The resistivity models from both inversions (see Fig. 5.7) were compared with the lithological data collected in existing boreholes, resistivity models from the inversion of cross-hole resistivity data and also water content models from Magnetic Resonance

Soundings (MRS). The electrical resistivity, the depth to the top and thickness of the water saturated zone is modeled more accurately with the 3D inversion (see Fig. 5.9). With the interpretation of the 3D electrical resistivity model, it is possible to make an estimate of the porosity variation in 3D to be used for transport modelling.

Considering the reasonably shorter RMT data acquisition time compared to a full 3D ERT survey, the method has a good potential to be utilized to image the near surface resistivity structures in 3D for monitoring purposes.

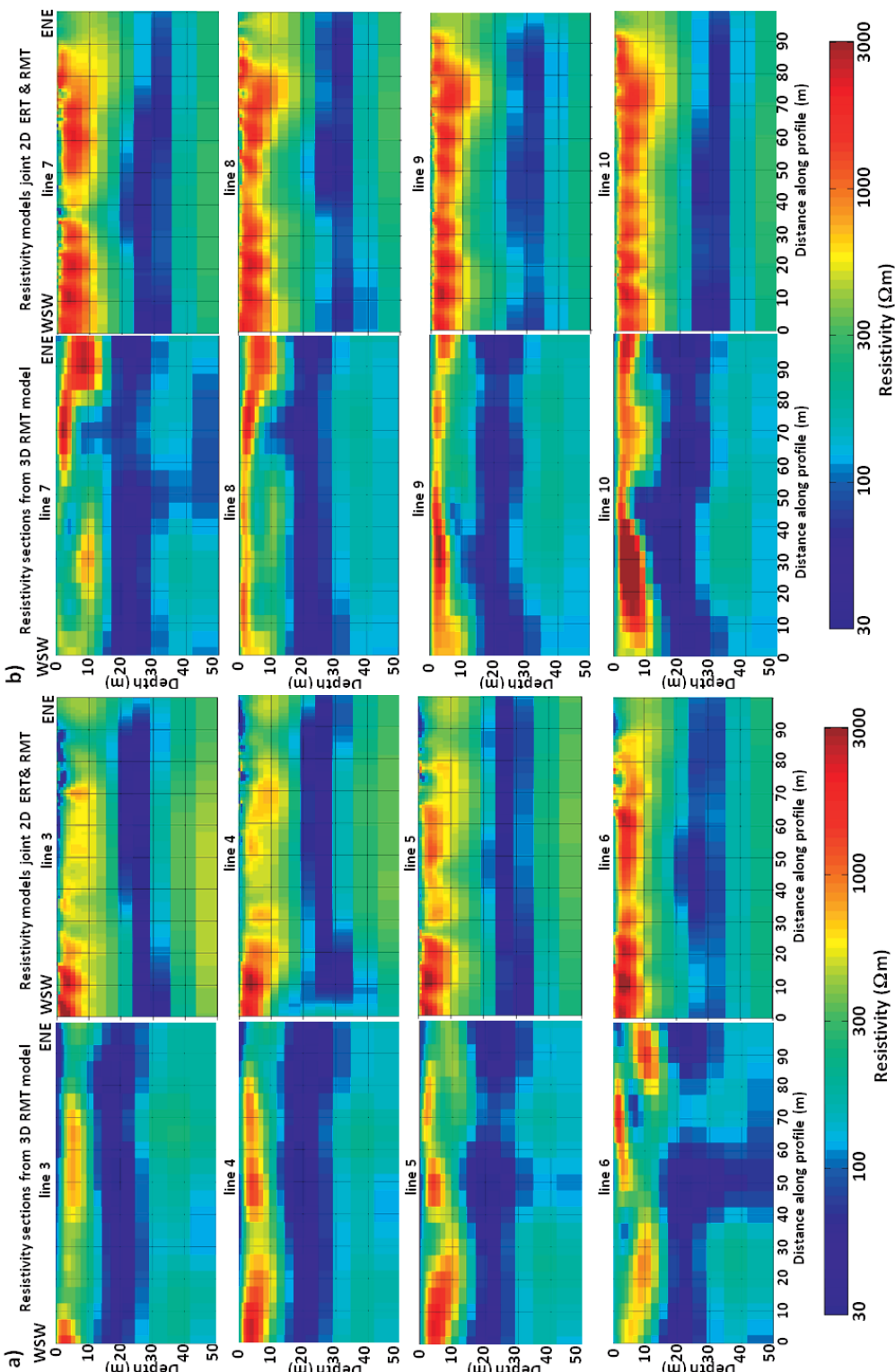


Figure 5.7. Comparison between the results from 3D inversion of RMT data (left panels) and 2D joint inversion of ERT and RMT data (right panels) collected in the Treceite site. Sections from 3D RMT resistivity model and resistivity models from 2D joint ERT and RMT data inversion a) along lines 3 to 6 and b) along lines 7 to 10.

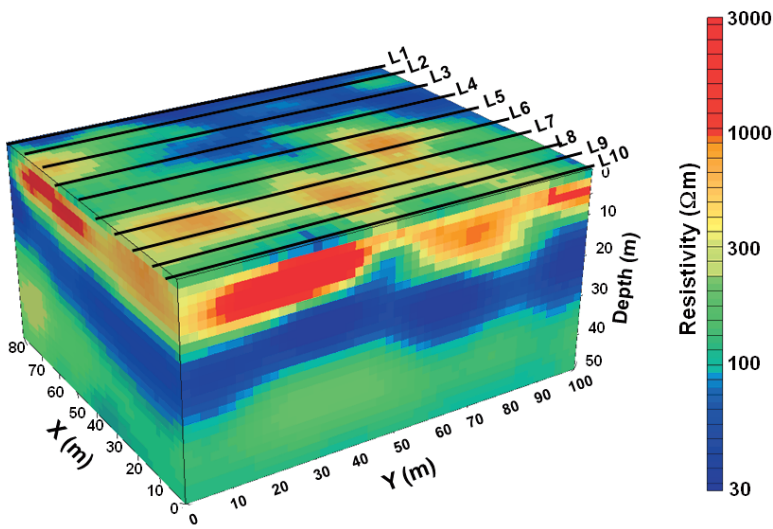


Figure 5.8. Resistivity model from 3D inversion of RMT data in the Trecate site.

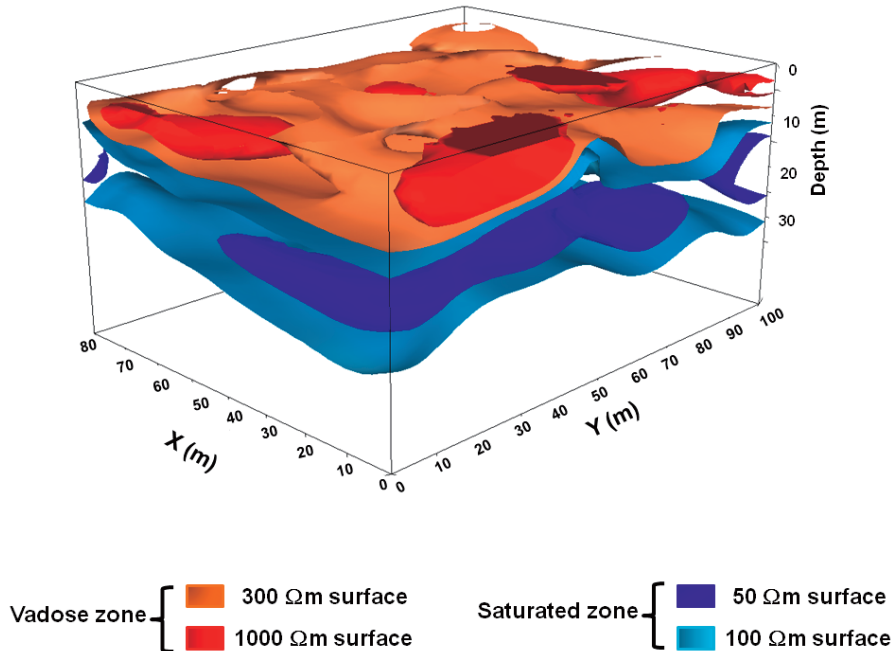


Figure 5.9. Morphology of the saturated and unsaturated zone estimated from 3D RMT resistivity model in the Trecate area.

6. Discussion and conclusions

In this thesis I present the results from two geophysical case studies involving magnetotelluric data inversion and interpretation. Both cases highlight the potential of 3D inversion of MT data to find the best possible representation of the electrical conductivity structure of the subsurface, but also illustrate that 3D inversion is still not a standard procedure.

In the study of the Skellefte ore district in northern Sweden, MT data was used to derive a crustal scale electrical conductivity model in 2D along selected profiles and successively in 3D of the Kristineberg area. Dimensionality analysis has revealed strong lateral changes in the area, where an overall geo-electrical strike direction could not be satisfactorily estimated. This eventually necessitated a 3D inversion approach. Data quality and site spacing were sub-optimal and the geological structure quite complex. Additional information was sparse on the crustal scale, where only reflection seismic data was available for comparison and model construction. Nevertheless, the 3D inversion model derived from MT data could provide valuable additional information for interpretation of the geological setting of the study area. The observed model features could be correlated with lithological units and together with seismic reflection images a consistent picture of the upper 12 km of the subsurface was derived. Especially the thickness of the overlying granitic intrusive rocks were consistently observed with both methods. Most prominent was a strong crustal conductivity anomaly at a depth that could be interpreted as a structural basement for the Bothnian basin sediments.

The second study presents results from an investigation of oil blow-out near Trecate, Italy. With the interpretation of densely sampled radiomagnetotelluric data, the vadose zone and underlying aquifer could be imaged in the upper 60 m in three dimensions, which is necessary for the monitoring of the remediation process and for setting up a general geohydrological model. At the same time, 2D joint inversion with existing electrical resistivity tomography data was performed and compared to the single 3D RMT model. The joint inversion benefits from the different sensitivities of both methods, where the 3D single inversion provided the best image of the aquifer in the whole study area. The presented results help addressing the geological questions they have been targeting.

Methodologically, 3D inversion should be further evaluated and developed. The transition from the now standard 2D to 3D MT data inversion can be compared with the development in the 1990's, when 2D inversion algorithms became widely available. The problematic issues in MT data interpretation

like distortion and resolution have been intensively studied ever since, assuming a 2D regional model even when not justified by the data. 3D inversion on the other hand is new terrain for geophysicists today and results need to be carefully analyzed before a geological interpretation is made. While dimensionality issues can finally be overcome, other issues have to be addressed, namely sufficiently dense data sampling and sufficiently fine model discretization to resolve the targeted structures. The effects of galvanic distortion in 3D need to be studied further.

New insights into the capabilities of 3D inversion of MT data have been gained within the two case studies, which represent very different applications of the magnetotelluric method. Frequency and depth range are on opposite ends of the magnetotelluric scale and data quality and sampling density are far better for the Trecate study, where also geological complexity is simpler and more additional information is available. Synthetic studies with 3D models for both areas confirmed the restrictions of 2D assumptions, where the inversion of the determinant was found to be a good compromise in a 3D environment. Some weaknesses of the used algorithms are the underestimation of the true resistivity of more resistive structures and the smearing effects of conductive features due to smoothing constraints in the inversion.

Outlook

In the future, the further development of 3D inversion algorithms will include distortion parameters as part of the model and possibly give the opportunity of different model discretization with e.g. finite elements. Fully parallel codes, able to solve bigger problems and to test finer meshes, will hopefully be made available to the EM community. Faster performance will allow more thorough model assessment. Systematic sensitivity analyses should be developed. Additionally, testing different optimization approaches to better determine strengths and weaknesses of certain algorithms would be beneficial. Finally, joint inversion with other data sets will fully use the potential of the MT method to help investigate the structure of the Earth.

Sammanfattning på svenska

Från 2D till 3D modeller av elektrisk ledningsförmåga baserad på magnetotelluriska data - erfarenheter från två fallstudier

Magnetotelluriska (MT) mätningar är bland de få geofysiska metoder som kan kartlägga både marknära strukturer så väl som hela jordskorpan. Med de senaste framstegen inom mätteknik och beräkningsmetodik har det blivit möjligt att beräkna tredimensionella (3D) inversa modeller av den elektriska ledningsförmågan från MT data. Därmed kan problematiken med att göra ett tvådimensionellt (2D) modellantagande för en 3D värld undvikas. Övergången från 2D till 3D kräver en noggrann omprövning av de klassiska utmaningarna inom magnetotellurik: galvanisk distorsion, datafel, modelldiskretisering och upplösningsförmåga. I mitt arbete presenteras två magnetotelluriska fallstudier där en ny 3D inversionsalgoritm har tillämpats. De nya modellerna jämförs med konventionella 2D modeller, samt resultaten från andra geofysiska metoder såsom reflektionsseismik och elektrisk resistivitetstomografi (ERT).

Artikel I beskriver en typisk 2D MT studie med en samlokalisering seismisk tolkning från Kristinebergsområdet i Skelleftefältet i norra Sverige. Mätdata samlades in på 20 stationer längs en 20 km lång profil, vinkelrätt mot en antagen geoelektrisk strykning. Efter en dimensionalitetsanalys utfördes en 2D inversmodellering och en stabil modell av den elektriska ledningsförmågan i de översta 12 km av jordskorpan kunde presenteras. Elektriska strukturer i modellen är korrelerade med olika zoner av seismisk reflektivitet och tolkas som litologiska enheter kända från ytobservationer. Resultaten ger viktiga ledtrådar till förståelsen av processerna som format Skelleftefältet som vi ser det idag.

Artikel II utvidgar undersökningen av Kristinebergsområdet med ytterligare MT mätningar, närmare gruvan, längs två vinkelräta ca. 10 km långa profiler. Vi stötte här på den typiska utmaningen med 2D antagandet: hur definierar man en gemensam geoelektrisk strykning? Grundlig dimensionalitetsanalys leder till slutsatsen att den underliggande resistivitetsfördelningen på-verkas av måttliga 3D-effekter. En 2D inversmodellering av determinant-data kan fortfarande producera rimliga resultat. Ett par mer svår-tolkade modelegenskaper studeras med olika modellbedömningstekniker, t.ex. hypotestestning. För att kvantifiera 3D effekter i datat utfördes en syntetisk 3D-studie.

Artikel III avslutar sedan de elektromagnetiska undersökningarna i Skelleftefältet genom att呈现出 en första 3D inversionsmodell av ett $20 \times 20 \text{ km}^2$

stort område runt Kristinebergsgruvan. Kvaliteten på datat och fördelningen av de totalt 68 mätstationerna är inte idealisk, men den framtagna modellen är rimlig efter en samtolkning med resultat från seismiska reflektionsmätningar och geologisk information insamlad i fält och i borrhål. Giltigheten av modellen evalueras med hjälp av direkt modellering och en jämförelse med tidigare resultat från 2D-inversmodellering.

Artikel IV tar oss till ett annat fältområde vid en olje-blow-out nära Trecate, Italien. Som del av en tvärvetenskaplig studie insamlades radiomagnetotelluriska (RMT) och ERT data över ett tätt rutnät, för att undersöka den omräntande zonen ovan grundvattenzonens i det kontaminerade området, samt den generella geometrin av akvifären. En syntetisk studie utfördes för att undersöka de bågge metodernas möjligheter och begränsningar, dels i en 3D RMT-inversmodellering och dels i en kombinerad 2D RMT- och ERT-modellering. De resulterande inversionsmodellerna belyser den roll som RMT mätningar kan spela i ett övervakningsprojekt. De presenterade resultaten bidrar till att belysa de geologiska frågeställningarna som föreligger.

Metodologiskt bör 3D inversmodellering ytterligare utvärderas och utvecklas. Övergången från den numera rutinmässiga 2D analysen till 3D-MT inversmodellering kan jämföras med utvecklingen under 1990-talet, när 2D-inversionsalgoritmer blev allmänt tillgängliga och ersatte 1D modelleringsmetoder. De problematiska aspekterna i MT modellering av data, som distorsion och upplösning, har studerats flitigt allt sedan 2D regionala modeller antagits (även då detta antagande varit i konflikt med datat). 3D inversmodellering å andra sidan är ny terräng för geofysiker idag och resultaten måste analyseras noga innan geologisk tolkning kan göras. Medan dimensionalitetsproblematiken äntligen kan övervinnas uppstår annan problematik som måste behandlas, nämligen att erhålla tillräckligt tät sampling och tillräckligt fin diskretisering av modellen för att uplösa de undersökta strukturerna i tillräcklig detalj. Effekterna av galvanisk distorsion i 3D behöver studeras ytterligare. Nya insikter om möjligheterna för 3D inversmodellering av MT data har erhållts från de två fallstudierna, vilka representerar mycket olika applikationer av den magnetotelluriska metoden. Frekvens och djupintervall i de två fallstudierna är från motsatta ändar på den magnetotelluriska skalan och datakvaliteten och stationsavståndet är långt bättre för Trecate studien än i Skelleftefältet. Där är även den geologiska komplexiteten mindre och den tillgängliga oberoende information större. Syntetiska studier med 3D modeller av bågge områden har bekräftat begränsningen av 2D antagandet, där inversmodellering av determinant-data har varit en bra kompromiss i en 3D-miljö. Några svagheter i de använda algoritmerna är underskattningen av den sanna resistiviteten i mera resistiva strukturer och utsmetningseffekter på grund av regulariseringen i inversmodelleringen.

I framtiden kommer den fortsatta utvecklingen av 3D-inversionsalgoritmer att inkludera distorsionsparametrar som en del av modellen och eventuellt ge möjlighet till olika modelldiskretiseringar, t.ex. med finita element. Helt

parallelala koder bör göras tillgängliga för EM samhället, för att kunna lösa större problem med bättre upplösning. Högre prestanda kommer att ge en mer grundlig modellbedömning. Vidare behöver systematiska känslighetsanalyser utvecklas. Det skulle dessutom vara fördelaktigt att testa olika optimeringsmetoder för att bättre avgöra styrkor och svagheter i vissa algoritmer. Slutligen kan en gemensam inversmodellering med andra mätdata till fullo utnyttja potentialen hos MT datat för att undersöka jordens struktur.

Acknowledgments

These last years here in Uppsala have been a tremendously rich experience both academically and socially. Here is the place to thank all those who helped me see that maybe resistance is futile, but resistivity is not:

Firstly to my main supervisor Laust B. Pedersen. Thank you for inviting me to Uppsala and always having an open door. I appreciate all the scientific freedom I had during my doctorate and all the extra lessons I learned about science and academia.

To Ari Tryggvason, for being a cooperative and compassionate second supervisor. Thanks especially for taking me on the field trip to Eyjafjallajökull, which had nothing to do with my PhD, but everything with being a geophysicist.

To Alireza Malehmir for giving me a quick start in doing applied geophysics and for pushing the first manuscript.

To Maxim Smirnov, who did not only teach me huge amounts on practical MT issues but also provided splendid fieldwork in Norway and northern Sweden. Thanks for all your super quick answers, bug fixes and the best mushroom soup I ever tried!

To Mehrdad Bastani: I very much enjoyed our cooperation and am thankful for all the things I learned about RMT from you.

To María García: You were the best companion I could hope finding here in the far north. Thanks for all the good times we had in the field, in the office, on project meetings, midsommar, skiing, igloo building etc.

To Lars Dynesius: “If you’re looking for trouble, you have to do EM”, well, in that respect you were always the best of practical help! Thanks for fixing all our broken instruments and never giving up on trouble.

To everyone in the EM group in Uppsala for fruitful discussions and academic assistance.

Thanks to the partners from the Vinnova 4D project from Boliden and Luleå, especially to the reflection seismic group and Christopher Juhlin, who involved his whole family in our field work. Furthermore to Tobias Bauer, Pietari Skyttä and Tobias Hermansson for never giving up explaining all the colorful geology in the Skellefte area.

My extensive thanks go to Peter Schmidt, who was the kindest of neighbors and a “most agreeable” office mate.

Thanks to all my friends from the MT-community who helped and greatly inspired me: Thomas Kalscheuer, Naser Mecqbel, Max Moorkamp, Wenke Wilhelms, Marion Miensopust, Anna Avdeeva, Alexandros Savvidis. It was

always a pleasure meeting up on conferences or seeing you on guest visits. I am thankful for all the travel stipends I received during my PhD years from Wallenberg and Liljewalchs foundations (Uppsala university), Otterborgska donationsfond (Geologiska sektionen), the University of the Faroe Islands and the National graduate school in scientific computing.

The technical staff is greatly appreciate for their work: Arnaud Pharasyne and Michael Schieschke for humorous assistance with the monster often referred to as computer. Taher Mazloomian, Siv Petterson, Leif Nyberg, Anna Callerholm, Ingegerd Ohlsson, Zara Witt-Strömer, Susanne Paul and Helene Lundgren for making things run smoothly at Geocentrum.

Working at Villavägen was always enjoyable with so merry a company as with people at *geofysik* (Azita, Björn, Chunling, Daniel, Emil, Eva, Hasse, Magnus, Monika, Nicoleta, Omid, Peter H., Sahar, Saeid, Yang, Zhang) and *berg* (Abigail, Alicja, Börje, Faramarz, Hongling, Jarek, Karin, Kirsten, Micha, Peter D., Steffi, Zhina) with *Orienten* as our melting pot. No question that fika was my favorite time of the working day when I could share it with you and learn about life from all those places you call home and to broaden my horizon on Swedish expressions and trivia.

Special thanks to “team crazy” Ester, Frances, Niklas and Jochen for our trips to Abisko and Spain and playing innebandy. To Lara for being good company when in misery and on a fantastic road trip through Sweden: “Keep calm and carry on!” will take us anywhere we want to go.

I don’t want to forget the “dark side of the moon” in *Luval* and *paleo*, thanks for mingling with us “nördts”: Agnes, Beatrix, Carmen, Diana, Martin, Lebing and Jorinjtje, Allison, Cissi and Barbro.

Big thanks to Anna Ladenberger and Chris Hieronymus for all the friendship, food and shelter!

A special thought goes to friends that were there in my first days in Uppsala and have now moved on: Kristin and Pálmi, Cedric, Nina, Artem and Lena, Zuzana.

To my Uppsala friends, to the guys who suffered through the Teacher Training course with me, to my neighbors and especially to the ones from the “shooting the sheriff”-club.

To my band mates in *phontrattarne* who really showed me what it is like to be “Ein Student aus Uppsala”.

Finally to my loved ones back on the “continent”: Thank you for holding on to me and being my home wherever I am.

Juliane Hübert,
December 2011

References

- Allen, R., Weiher, P., Svenson, S., 1996. Setting of Zn-Cu-Au-Ag Massive Sulphide Deposits in the Evolution and Facies Architecture of a 1.9 Ga Marine Volcanic Arc, Skellefte District, Sweden. *Economic Geology* 91, 1022–1053.
- Avdeev, D., 2005. Three-dimensional electromagnetic modelling and inversion from theory to application. *Surveys in Geophysics* 26, 767–799.
- Avdeev, D., Kuvshinov, A., Pankratov, O., Newman, G., 2002. Three-dimensional induction logging problems, Part I: An integral equation solution and model comparisons. *Geophysics* 67 (2), 413–426.
- Bahr, K., 1991. Geological noise in magnetotelluric data: a classification of distortion types. *Physics of The Earth and Planetary Interiors* 66 (1-2), 24 – 38.
- Bastani, M., 2001. EnviroMT - a new Controlled Source/Radio Magnetotelluric System. Ph.D. thesis, Uppsala University.
- Bastani, M., Pedersen, L., 2001. Estimation of magnetotelluric transfer functions from radio transmitters. *Geophysics* 66 (4), 1038–1051.
- Bauer, T., Skyttä, P., Allen, R. L., Weiher, P., 2011. Syn-extensional faulting controlling structural inversion: Insights from the Palaeoproterozoic Vargfors syncline, Skellefte mining district, Sweden. *Precambrian Research* 191 (3-4), 166 – 183.
- Becken, M., Pedersen, L., 2003. Transformation of VLF anomaly maps into apparent resistivity and phase. *Geophysics* 68 (2), 497–505.
- Bedrosian, P., 2007. MT+, Integrating Magnetotellurics to Determine Earth Structure, Physical State, and Processes. *Surveys in Geophysics* 28, 121–167.
- Bergström, U., 2001. Geochemistry and tectonic setting of volcanic units in the northern Västerbotten country, northern Sweden. *Economic Geology Research* 1, C 833, 69–92.
- Boerner, R.-U., Ernst, O. G., Spitzer, K., 2008. Fast 3-D simulation of transient electromagnetic fields by model reduction in the frequency domain using Krylov subspace projection. *Geophysical journal international* 173 (3), 766–780.
- Bondeson, A., Rylander, T., Ingelström, P., 2005. Computational electromagnetics. Springer.
- Cagniard, L., 1953. Basic theory of the magnetotelluric method. *Geophysics* 18, 605–635.
- Cassiani, G., Strobbia, C., Gallotti, L., 2004. Vertical radar profiles for the characterization of deep vadose zones. *Vadose Zone Journal* 3, 1093–1105.
- Constable, S., Parker, R., Constable, C., 1987. OCCAMs inversion - A practical algorithm for generating smooth models from electromagnetic sounding data. *Geophysics* 52 (3), 289–300.
- Dahlin, T., Zhou, B., APR 2006. Multiple-gradient array measurements for multichannel 2D resistivity imaging. *Near surface geophysics* 4 (2), 113–123.

- Dehghannejad, M., Juhlin, C., Malehmir, A., Skytta, P., Weiher, P., 2010. Reflection seismic imaging of the upper crust in the Kristineberg mining area, northern Sweden. *Journal of applied geophysics* 71 (4), 125–136.
- Ernstson, K., Kirsch, R., 2006. Geoelectrical methods. In: Kirsch, R. (Ed.), *Groundwater Geophysics*. Springer Berlin Heidelberg, pp. 85–117.
- Gaal, G., Gorbatshev, R., 1987. An outline of the Precambrian evolution of the Baltic Shield. *Precambrian Research* 35, 15–52.
- García Juanatey, M. d. l. A., Hübner, J., Tryggvason, A., Pedersen, L. B., 2011. Imaging the Kristineberg mining area with two perpendicular magnetotelluric profiles in the Skellefte Ore District, northern Sweden. in press at *Geophysical prospecting*.
- Hutton, R., Haak, V., 1991. Special issue - high conductivity layers in the crust and upper mantle - evidence from field and laboratory measurements - preface. *Physics of the Earth and Planetary Interiors* 66 (1-2), ix –.
- Jones, A. G., 1998. Waves of the future: Superior inferences from collocated seismic and electromagnetic experiments. *Tectonophysics* 286, 273–298.
- Juhlin, C., Elming, S.-A., Mellqvist, C., Öhlander, B., Weiher, P., Wikström, A., 2002. Crustal reflectivity near the Archaean-Proterozoic boundary in northern Sweden and implications for the tectonic evolution of the area. *Geophys. J. Int.* 150, 180–197.
- Kalscheuer, T., Juanatey, M. d. l. A. G., Meqbel, N., Pedersen, L. B., 2010. Non-linear model error and resolution properties from two-dimensional single and joint inversions of direct current resistivity and radiomagnetotelluric data. *Geophysical Journal International* 182 (3), 1174–1188.
- Lahti, I., Korja, T., Kaikkonen, P., Vaittinen, K., Grp, B. W., DEC 2005. Decomposition analysis of the BEAR magnetotelluric data: implications for the upper mantle conductivity in the Fennoscandian Shield. *Geophysical Journal International* 163 (3), 900–914.
- Loke, M., Barker, R., 1996. Rapid least-squares inversion of apparent resistivity pseudosections by a quasi-Newton method. *Geophysical prospecting* 44 (1), 131–152.
- Malehmir, A., Thunehed, H., Tryggvason, A., 2009. The Paleoproterozoic Kristineberg mining area, northern Sweden: Results from integrated 3D geophysical and geologic modeling, and implications for targeting ore deposits. *Geophysics* 74 (1), B9–B22.
- Malehmir, A., Tryggvason, A., Lickorish, H., Weiher, P., 2007. Regional structural profiles in the Western part of the Paleoproterozoic Skellefte Ore District, northern Sweden. *Precambrian Res.* 159, 1–18.
- Menke, W., 1984. *Geophysical Data Analysis: Discrete Inverse Theory*. Vol. 45. International Geophysics Series.
- Moorkamp, M., Heincke, B., Jegen, M., Roberts, A. W., Hobbs, R. W., JAN 2011. A framework for 3-D joint inversion of MT, gravity and seismic refraction data. *Geophysical Journal International* 184 (1), 477–493.
- Newman, G. A., Recher, S., Tezkan, B., Neubauer, F. M., 2003. 3D inversion of a scalar radio magnetotelluric field data set. *Geophysics* 68 (3), 791–802.
- Nolasco, R., Tarits, P., Filloux, J., Chave, A., 1998. Magnetotelluric imaging of the Society Islands hotspot. *Journal of Geophysical Research-Solid Earth* 103 (B12),

30287–30309.

- Park, S., Mackie, R., 2000. Resistive (dry?) lower crust in an active orogen, Nanga Parbat, northern Pakistan. *Tectonophysics* 316 (3-4), 359–380.
- Pedersen, L. B., Bastani, M., Dynesius, L., 2006. Radiotransmitters in Europe and their use in high resolution geophysical exploration of near-surface geology. *Geophysics* 71 (6), G279–G284.
- Pedersen, L. B., Engels, M., 2005. Routine 2D inversion of magnetotelluric data using the determinant of the impedance tensor. *Geophysics* 70, G31–G41.
- Pellerin, L., Hohmann, G. W., 1990. Transient electromagnetic inversion: A remedy for magnetotelluric static shifts. *Geophysics* 55, 1242–1250.
- Årebäck, H., Barret, T., Abrahamsson, S., Fagerström, P., 2005. The Palaeoproterozoic Kristineberg VMS deposit, Skellefte district, northern Sweden, part I: geology. *Mineralium Deposita* 40, 351–367.
- Rutland, R., Kero, L., Nilsson, G., Stolen, L., 2001. Nature of a major tectonic discontinuity in the Svecocambrian province of northern Sweden. *Precambrian Research* 112, 211–237.
- Schmucker, U., Weidelt, P., 1975. Electromagnetic induction in the earth. In: *Lectures Notes Aarhus 1975*. Laboratoriet for anvendt geofysik, Aarhus Universitet.
- Schwalenberg, K., Rath, V., Haak, V., 2002. Sensitivity studies applied to a two-dimensional resistivity model from the Central Andes. *Geophysical Journal International* 150 (3), 673–686.
- Singer, B. S., 1992. Correction for distortions of magnetotelluric fields: Limits of validity of the static approach. *Surveys in Geophysics* 13, 309–340, 10.1007/BF01903482.
- Siripunvaraporn, W., Egbert, G., 2000. An efficient data-subspace inversion method for 2D magnetotelluric data. *Geophysics* 65, 791–803.
- Siripunvaraporn, W., Egbert, G., 2009. Wsinv3dmt: Vertical magnetic field transfer function inversion and parallel implementation. *Physics of the Earth and Planetary Interiors* 173 (3-4), 317 – 329.
- Siripunvaraporn, W., Egbert, G., Lenbury, Y., Uyeshima, M., 2005. Three-dimensional magnetotelluric inversion: data-space method. *Physics of the Earth and Planetary Interiors* 150 (1-3), 3–14.
- Skyttä, P., Hermansson, T., Andersson, J., Whitehouse, M., Weiher, P., 2011. New zircon data supporting models of short-lived igneous activity at 1.89 ga in the western skellefte district, central fennoscandian shield. *Solid Earth* 2 (2), 205–217.
- Skyttä, P., Hermansson, T., Elming, S., Bauer, T., 2010. Magnetic fabrics as constraints on the kinematic history of a pre-tectonic granitoid intrusion, kristineberg, northern sweden. *Journal of Structural Geology* 32 (8), 1125 – 1136.
- Smirnov, M., 2003. Magnetotelluric data processing with a robust statistical procedure having a high breakdown point. *Geophysical Journal International* 152, 1–7.
- Smirnov, M., Korja, T., Dynesius, L., Pedersen, L. B., Laukkanen, E., 2008. Broadband Magnetotelluric Instruments for Near-surface and Lithospheric Studies of Electrical Conductivity: A Fennoscandian Pool of Magnetotelluric Instruments. *Geophysica* 44(1-2), 31–44.

- Smirnov, M. Y., Pedersen, L., 2009. Magnetotelluric measurements across Sorgenfrei-Tornquist-zone in southern Sweden and Denmark. *Geophysical Journal International* 176, 443–456.
- Swift, C. M., 1967. A magnetotelluric investigation of electrical conductivity anomaly in the southwestern united states. PhD Thesis Massachusetts Institute of Technology.
- Telford, W. M., Geldart, L. P., Sheriff, R. E., 1990. Applied geophysics. Cambridge University Press.
- Tikhonov, A. N., 1950. On determining electrical characteristics of the deep layers of the Earth. *Dokl. Akad. Nauk. SSSR* 73, 295–297.
- Tryggvason, A., Malehmir, Juhlin, C., Rodriguez-Tablante, J., Weiher, P., 2006. Seismic reflection investigation in the western part of the Palaeoproterozoic Skellefte Ore District, northern Sweden. *Economic Geology* 101, 1039–1054.
- Weiher, P., Bergman, J., Bergström, U., 1992. Metallogeny and tectonic evolution of the Early Proterozoic Skellefte District, northern Sweden. *Precambrian Research* 58, 143–167.
- Wiese, H., 1962. Geomagnetische Tiefentellurik Teil II: die Streichrichtung der Untergrundstrukturen des elektrischen Widerstands, erschlossen aus geomagnetischen Variationen. *PAGEOPH*, 83–103.
- Zhang, P., Roberts, R.G., Pedersen, L., 1987. Magnetotelluric Strike Rules. *Geophysics* 52, 267–278.
- Zhdanov, M. S., Green, A., Gribenko, A., Cuma, M., 2010. Large-Scale Three-Dimensional Inversion of EarthScope MT Data using the Integral Equation Method. *Physics of the Solid Earth* 46, 670–678.

Acta Universitatis Upsaliensis

*Digital Comprehensive Summaries of Uppsala Dissertations
from the Faculty of Science and Technology 890*

Editor: The Dean of the Faculty of Science and Technology

A doctoral dissertation from the Faculty of Science and Technology, Uppsala University, is usually a summary of a number of papers. A few copies of the complete dissertation are kept at major Swedish research libraries, while the summary alone is distributed internationally through the series Digital Comprehensive Summaries of Uppsala Dissertations from the Faculty of Science and Technology.

